Design and Performance Investigation of Liquid based cooling system for Electrical converter system of Adama I wind power plant

Hailu Desalegn Tagelu

A Thesis submitted to the Department of Mechanical Engineering

School of Mechanical, Chemical & Materials Engineering

Presented in Partial Fulfillment of the Requirement for the Degree of Master of Science in Thermal Engineering

Office of Graduate studies

Adama Science and Technology University

July, 2024 G.C

Adama, Ethiopia

Design and Performance Investigation of Liquid based cooling system for Electrical converter system of Adama I wind power plant

Hailu Desalegn Tagelu

Advisor: Dr. Addisu Bekele (Associate Professor)

A Thesis submitted to the Department of Mechanical Engineering

School of Mechanical, Chemical & Materials Engineering

Presented in Partial Fulfillment of the Requirement for the Degree of Master in Thermal Engineering

Office of Graduate Studies

Adama Science and Technology University

July, 2024 G.C

Adama, Ethiopia

DECLARATION

I hereby declare that this thesis entitled "Design and Performance Investigation of Liquid based cooling system for Electrical converter system of Adama I wind power plant" is my original work. That is, it has not been submitted for the award of any academic degree, diploma or certificate in any other university. All sources of materials that are used for this thesis have been duly acknowledged through citation.

Hailu Desalegn Tagelu	________________________	_______________
Name of Student	Signature	Date

RECOMMENDATION OF ADVISOR

I, the advisor of this thesis, hereby certify that I have read the revised version of the thesis entitled "Design and Performance Investigation of Liquid based cooling system for Electrical converter system of Adama I wind power plant" prepared under my guidance by Hailu Desalegn Tagelu submitted in partial fulfillment of the requirements for the degree of Master of Science in Thermal Engineering. Therefore, I recommend the submission of revised version of the thesis to the department following the applicable procedures.

Dr. Addisu Bekele	________________________	_______________
Advisor	Signature	Date

APPROVAL PAGE

I, the advisor of the thesis entitled "Design and Performance Investigation of Liquid based cooling system for Electrical converter system of Adama I wind power plant" and developed by Hailu Desalegn Tagelu hereby certify that the recommendation and suggestions made by the board of examiners are appropriately incorporated into the final version of the thesis.

Dr. Addisu Bekele	________________________	________________
Advisor	Signature	Date

We, the undersigned, members of the Board of Reviewers of the thesis by Hailu Desalegn Tagelu have read and evaluated the thesis entitled "Design and Performance Investigation of Liquid based cooling system for Electrical converter system of Adama I wind power plant" and examined the candidate during open defense. This is, therefore, to certify that the thesis is accepted for partial fulfilment of the requirement of the degree of Master of Science in Thermal Engineering.

Chairperson	Signature	Date
Internal Examiner	Signature	Date
External Examiner	Signature	Date

Final approval and acceptance of the thesis is contingent upon submission of its final copy to the Office of Postgraduate Studies (OPGS) through the Department Graduate Council (DGC) and School Graduate Committee (SGC).

Department Head	Signature	Date
School Dean	Signature	Date
Office of Postgraduate Studies, Dean	Signature	Date

ACKNOWLEDGEMENT

I would like to express my deepest gratitude to almighty God for his endless love. I am grateful to my Advisor Dr. Addisu Bekele (Associate Professor) for his invaluable guidance. Thanks should also go to my wife, class mates as well as Adama I Wind Power Plant Maintenance & Operation staff members for their cooperation and for being part of this important milestone in my Academic path.

TABLE OF CONTENT

ACKNOWLEDGEMENT I

LIST OF FIGURES VI

ACRONYM IX

ABSTRACT X

CHAPTER ONE 1

INTRODUCTION 1

1.1. Background of the study 1

1.1.1. Introduction to Converter system in Adama I WPP 1

1.1.2. Existing converter cooling system in the plant 3

1.1.3. Drawbacks of Forced Air Converter cooling system in Adama I 5

1.1.4. Direct contact single Phase Liquid Cooling 6

1.1.5. Structures of Liquid cooled Heat sinks 6

1.1.6. Flow Distribution of Liquid cooled heat sinks 7

1.1.7. Cold End of the working fluid (Heat Exchanger) 7

1.2. Statement of the problem 8

1.3. Research Hypothesis 9

1.4. General Objective 9

1.5. Specific Objective 9

1.6. Significance of the study 9

1.7. Limitation of the study 9

1.8. Operational Definition 10

CHAPTER TWO 12

LITERATURE REVIEW 12

2.1. IGBT Cooling 12

2.2. Liquid cooled Heat sinks 12

2.3. Research gaps 17

CHAPTER THREE 20

MATERIALS AND METHODS 20

3.1. Data Collection 20

3.1.1. Name Plates 20

3.1.2. Maintenance manuals & User manuals 20

3.1.3. SCADA 20

3.1.3. Actual measurement 20

3.2. Article reviews, Data sheets and Books 21

3.3. Data Analysis 21

3.3.1. Mathematical Modeling 21

3.3.2. Geometry Design 21

3.3.3. Numerical Simulation 21

3.3.4. Validation work 22

3.4. Document Compilation and Submission 22

CHAPTER FOUR 23

DESIGN OF THE SYSTEM AND NUMERICAL MODELING 23

4.1. General 23

4.2. Fluid flow type 24

4.3. Mathematical Modeling 26

4.3.1. Conservation of Mass (Continuity Equation) 26

4.3.2. Conservation of Momentum 26

4.3.3. Energy Equation 26

4.3.3. Heat Transfer along the Solid (Heat Sink) 27

4.3.4. Heat Transfer between the Heat sink and coolant 27
4.4. Numerical Modeling 27
4.4.1. Geometry Creation 28
4.4.2. Meshing 29
4.4.3. Grid Independence test 30
4.4.4. Numerical simulation setup 32
4.4.5. Numerical Model 32
4.4.6. Materials 32
4.4.7. Cell zones and Boundary conditions 33
4.4.8. Solution Methods, Initialization and Calculation 34
CHAPTER FIVE 35
RESULTS AND DISCUSSIONS 35
5.1. Numerical Study of Heat sink Thermal Property with different liquids 35
5.1.1. Average Heat sink Temperature 35
5.1.2. Heat sink average Temperature distribution along fluid flow direction 37
5.2. Volume Average Heat Sink Temperature 39
5.3. Analysis of Selected coolant (Water) with different Inlet Velocities 40
5.3.1. Heat Sink Temperature Comparison at different inlet velocities 40
5.3.2. Temperature Distribution of the fluid 45
5.4. Comparison of Water cooled Heat sink with Air cooled Heat sink 48
5.6. Collector Design 52
5.6.1. Fluent setup and input parameters for collector Analysis 53
5.6.2. Collector Analysis Results 54
5.7. Return Pipe Design 57
5.8. Cold end Heat Exchanger Sizing 58

5.8.1. Heat Exchangers in General 58
5.6.2. Selection of Condenser Heat Exchanger 59
5.9. Pump Selection 61
CONCLUSION AND RECOMENDATIONS 62
Conclusion 62
Recommendation(s) 63
REFERENCES 64
APPENDIX 67

LIST OF TABLE

Table 1.1. converter cooling related faults (from SCADA) 5
Table 2.1. Summary of literature review 18
Table 2.2. Concluding points from Literature review 19
Table 4.1. Variation of Heat sink average top surface Temperature with Mesh size 31
Table 4.2. Solid and Fluid materials with their properties 33
Table 4.3. Boundary conditions of the system 34
Table 5.1. Summary of Water cooled Heat sink comparison at different velocities 47
Table 5.2. Summary of Comparison of Air cooled Heat Sink Vs Water cooled Heat sink 51
Table 5.3. Recommended upper limits for ions in cooling water 52
Table 5.4. Input Parameters for collector Analysis 53
Table 5.5. Fluent setup for collector Analysis 54
Table 5.6. Input Parameters for Pipe Analysis 57
Table 5.7. Fluid properties for heat Exchanger sizing 59

LIST OF FIGURES

Figure 1.1. Adama I WPP Turbine system structure map (Gold Wind, 2011) 1
Figure 1.2. IGBT Module without protection components (SEMIKRON, 2017) 2
Figure 1.3. Front and side view of IGBT set (SEMIKRON, 2017) 3
Figure 1.4. Converter Cabinet picture 4
Figure 1.5. liquid cooled Heat sink structures 6
Figure 1.6. Coolant inlet outlet positions and manifold structure 7
Figure 1.7. Proposed system layout 11
Figure 3.1. Overall work Methodology 22
Figure 3.2. Numerical Work Procedure 28
Figure 4.1. Complete system Setup of the Liquid based Converter cooling 23
Figure 4.2. IGBT/DIODE set with collector 24
Figure 4.3. Geometry of the Heat sink 29
Figure 4.4. Mesh display of the geometry 30
Figure 4.5. Grid Independence test 31
Figure 5.1. Average Temperature distribution along the Heat Sink height with different fluids (at Vin = 0.8m/s) 35
Figure 5.2. Average Temperature distribution along the Heat Sink height with different fluids (at Vin = 0.6m/s) 36
Figure 5.3. Average Temperature distribution along the Heat Sink height with different fluids (at Vin = 0.4m/s) 37
Figure 5.4. Flow Direction Heat sink Average Temperature comparison at Vin = 0.8m/s 37
Figure 5.5. Flow Direction Heat sink Average Temperature comparison at Vin = 0.6m/s 38
Figure 5.6. Flow Direction Heat sink Average Temperature comparison at Vin = 0.4m/s 38
Figure 5.7. Heat Sink Volume Average Comparison at Vin = 0.8m/s 39
Figure 5.8. Heat Sink Volume Average Comparison at Vin = 0.6m/s 39
Figure 5.9. Heat Sink Volume Average Comparison at Vin = 0.4m/s 40
Figure 5.10. Vertical Heat Sink Average Temperature variation at different inlet velocities 41
Figure 5.11 Heat sink Temperature Contour (V_{in} = 0.8m/s) 42
Figure 5.12. Heat sink Temperature Contour (V_{in} = 0.6m/s) 42
Figure 5.13. Heat sink Temperature Contour (V_{in} = 0.4m/s) 43

Figure 5.14. Flow direction Heat sink Average Temperature distribution 43
Figure 5.15. Temperature Contour along the flow direction a) Vin = 0.8m/s b) Vin = 0.8m/ c) Vin = 0.8m/ 44
Figure 5.16. Temperature contour of a) fluid domain b) fluid at outlet (Vin = 0.8m/s) 46
Figure 5.17. Temperature contour of a) fluid domain b) fluid at outlet (Vin = 0.6m/s) 46
Figure 5.18. Temperature contour of a) fluid domain b) fluid at outlet (Vin = 0.4m/s) 47
Figure 5.19. Vertical Average Temperature distribution of Air cooled Heat sink 48
Figure 5.20. Air cooled Heat sink Temperature contour 49
Figure 5.21. Flow direction average Temperature distribution of Air cooled Heat sink 49
Figure 5.22. Flow direction Air cooled Heat sink Temperature contour 50
Figure 5.23. Fluid domain Temperature contour of Air cooled Heat sink 50
Figure 5.24. Fluid (Air) outlet temperature 51
Figure 5.25. Boundary conditions of Collector 55
Figure 5.26. Velocity path line of Collector 56
Figure 5.27. velocity vector of fluid flow inside collector 56
Figure 5.28. Return Pipe Geometry 58

ACRONYM

^0C	Degree Celsius
A	Area
AC	Alternating Current
CFD	Computational Fluid Dynamics
DC	Direct Current
ETB	Ethiopian Birr
h	Height
Hz	Hertz
IGBT	Insulated Gate Bipolar Transistor
IPM	Intelligent Power Module
KV	Kilo Volt
KW	Kilo Watt
Q	Heat Transfer Rate
LMTD	Log mean temperature difference
SCADA,	Supervisory control and data acquisition
v	Velocity
V	Volt
VFD	Variable Frequency Drive
w	Width
WPP	Wind Power Plant

ABSTRACT

This paper presents design and numerical performance investigation of single phase direct liquid cooling for Converter system of Adama I wind power plant. The cooling system design was done by applying liquid to the heat sink of Insulated Gate Bipolar Transistors (IGBTs) and rectifier Diodes. In Adama I, converter system consists a total of 10 IGBTs and 2 Diodes in two cabinets. The Heat sink of these IGBTs have 360 x 215 x 70 mm rectangular dimension and exposed to 30 W/Cm^2 heat flux at its top surface. Issues related to effectiveness, dust accumulation and reliability of the current forced air converter cooling is the motivation to propose liquid cooling. Single phase direct contact liquid cooling is reliable thermal management approach as it allows high heat exchange by conduction. In this study the model of liquid cooled IGBT and Diode heat sink was simulated by ANSYS fluent by considering steady state heat transfer and fluid flow. Three different fluids (Water, Glycol water mixture and Natural Oil) cooling performance was compared at three different inlet velocities (0.4, 0.6 & 0.8m/s). Water was found as best cooler to operate at 0.8m/s. Using water at 0.8m/s flow velocity and 25^0C inlet temperature lowered the heat sink's volume average temperature to 31.17^0C. Its top surface average and maximum temperature were 47.88^0C and 63.9^0C respectively. The target body's (heat sink's) Temperature when cooled by water was compared with that of the existing air cooling. 42.02^0C, 65.73^0C and 90.69^0C were heat sink volume average, top wall average and top surface maximum temperatures.

Key words: - *Converter system, Heat sink, IGBT, Liquid cooling, Numerical Simulation, Wind Turbine*

CHAPTER ONE

INTRODUCTION

1.1. Background of the study

1.1.1. Introduction to Converter system in Adama I WPP

The Electric Power generated by direct drive wind turbines like that of Adama I wind power plant enables efficient conversion of variable frequency and voltage (due to variable wind speed) to a fixed frequency and voltage that matches the grid system. Adama I wind power plant operates 34 wind turbines with 1.5 MW single turbine capacities. A single turbine generates a rated voltage of 620V AC at 12m/s or above wind speed. Since the turbines are direct drive type there is no gear box and the energy generated depends on the rotation of the generator rotor. In order to synchronize this variation with that of grid, a converter system is used in each turbine.

The converter system has diode rectifier, boost DC/DC converter and inverter as its main components. Two Diodes rectify AC produced by the turbine generator that has voltage of 0 ~ 620V AC and frequency 0 ~ 12.7 Hz to DC. Three IGBTs performs an action of DC to DC chopping, Finally Six IGBTs invert the DC power in to AC matching the voltage (620V), frequency (50Hz) and phase (3 phases) of the grid. The rest IGBT will perform breaking or discharging action during voltage picks on DC bus bar. After synchronization is achieved a unit transformer (620V/33KV) installed near each turbine will step up the voltage and it is finally transmitted to substation.

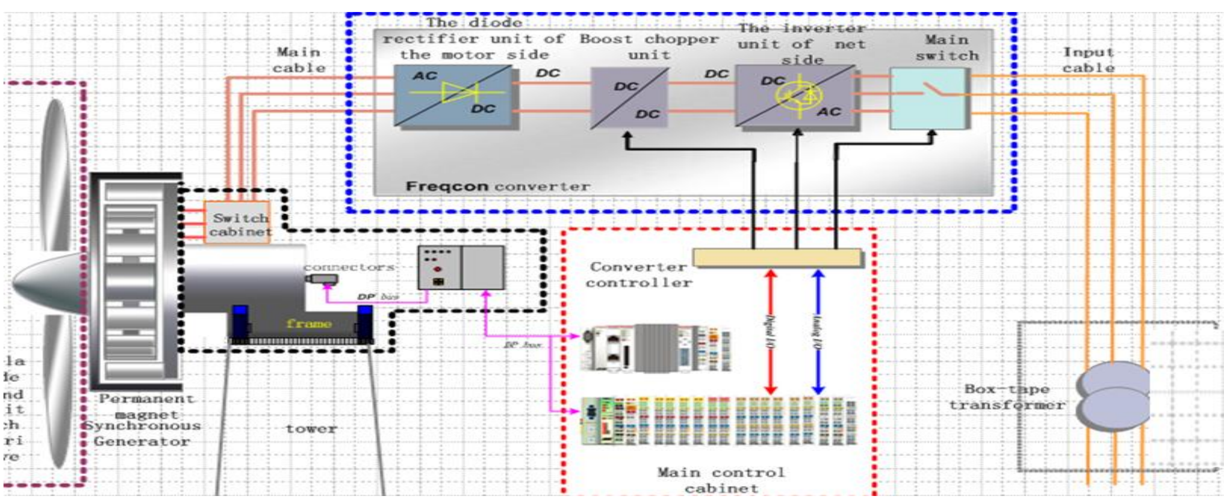

Figure 1.1. Adama I WPP Turbine system structure map (Gold Wind, 2011)

The IGBT set has an Intelligent Power Module (IPM) with high power density and reliability.

Heat sink, Gate drive, power stage drive and circuit board for protection are imbedded with the IBM module. The fluids used for cooling the heat sink part of the module are air, water and water and glycol mixture. One IGBT or Diode set has an overall dimension of (H x W x L) 820 x 620 x 430mm. 10 IGBT sets with 2 Diode sets forms the whole Converter system in a single turbine. They are grouped in to two cabinets (SEMIKRON International, 2017).

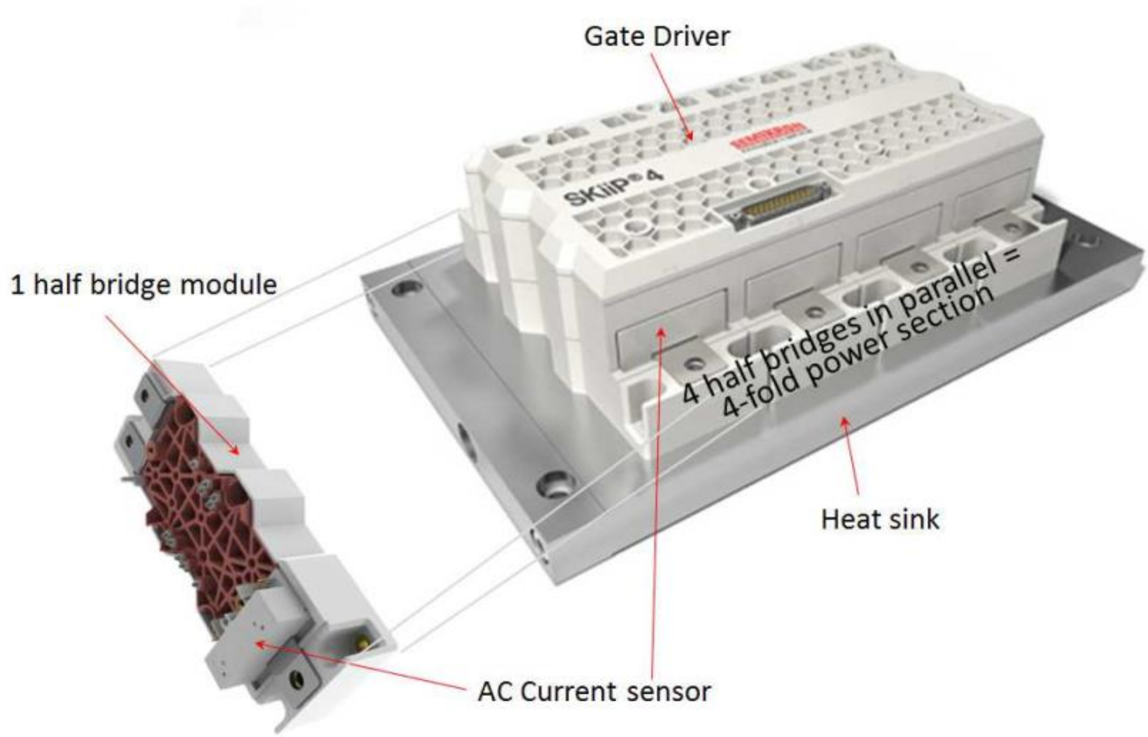

Figure 1.2. IGBT Module without protection components (SEMIKRON, 2017)

Each converter IGBTs and Diodes will reach 30 W/cm^2 of heat-flow density. The operating temperature of these sets highly affects their reliability. According to the manufacturer manual, an increase in Temperature by 1℃ in the range of 70-80℃ results in reduction of Reliability by 5%.

Each set of IGBT or Diode has an allowable maximum operating core Temperature of 100℃ with a temperature rise of 60℃. The cabinet is allowed to allowable ambient temperature up to 40℃. The Heat sink has a Temperature of 70℃ just 2mm below top Heat sink surface.

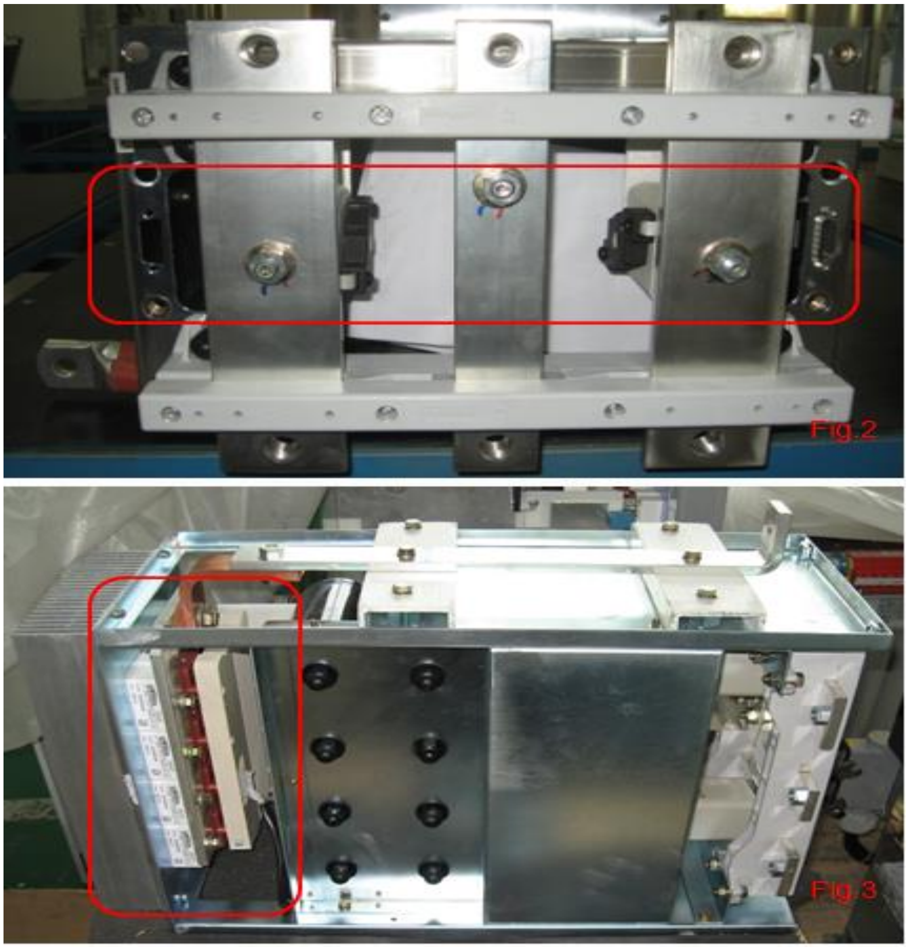

Figure 1.3. Front and side view of IGBT set (SEMIKRON, 2017)

1.1.2. Existing converter cooling system in the plant

IGBT module will produce high switching loss and on-state loss in the process of opening and closing, and the loss will be converted and accumulated in the form of heat. The compact structure and high power density of converters, especially the power cabinets installed with IGBT power modules, often lead to unforeseen device overheating risk and reliability problems, and even affect the of product development progress (Fei Yang et al., 2021).

Currently Adama I Converter system uses forced air cooling to meet the requirements of the operation temperature range between -30℃ to 40℃. On the top of the IGBT cabinet, a cooling fan is installed and controlled by Variable Frequency Drive (VFD). The cooling fan is started when the converter is started and regulates according to temperature received by VFD.

The draw backs of this Active cooling highly influence the performance of an electrical system. For example, as dust is accumulated, the converters (IGBTs) will overheat and get challenge to maintain its core temperature. There is also a DC bus bar inside the cabinet which is a DC conductor. The dust from outside of the cabinet will also affect it by acting as an insulating blanket. Evidence shows that these dust particles cause electric contact failures which seriously influence the reliability of electronic systems (Jih Gao Zhang, 1986).

The noisy operation of the cooling fans may lead to hearing problems. Even though it is designed near to the normal human hearing ability range, Maintenance and inspection works that needs to spend long and repetitive time will expose maintenance personnel to this noise. Need of more maintenance time and budget, high electric power consumption of the system, inability to achieve the desired temperature due to ambient air fluctuation and other running costs makes the existing cooling system challenging.

Figure 1.4. Converter Cabinet picture

1.1.3. Drawbacks of Forced Air Converter cooling system in Adama I

As the service year of the wind farm increases the cooling system related turbine failures are dramatically increasing. The IGBTs are the most frequently failed converter system components due to temperature fluctuation. The forced air cooling system can't achieve thermal stability during hot times and stressed system operation times. Electronic components on IGBT sets like resistors, diodes and capacitors fail to operate when the temperature of the set is beyond the limit.

Table 1.1. shows faults that are only referred as (quoted as temperature problem, unsymmetric etc.) converter cooling system problem collected from SCADA. The consequence of these faults is IGBT set failure which in turn leads to high spare part expense and maintenance work. The SCADA records fault history for those turbines whose communication is not interrupted (are being monitored remotely).

Table 1.1. converter cooling related faults (from SCADA)

Year	Number of faults (directly related to cooling)	Total number of turbines on which the faults occur	Total machine down time	
			In Hours	In days
2022	980	9	455:41:52	18.9 days
2021	298	8	258:13:32	10 days
2020	52	5	5:16:30	0.215 day
2019	47	6	24:14:04	1 day

The top three converter system faults are namely:

- IGBT Temperature Unsymmetric
- Fan feedback loss
- Over Temperature

IGBT and Diode sets can also stop their operation due to excessive dust and dirt accumulation on them. The source of these dusts is the ambient air that is forced to the cabinet for cooling purpose.

During Preventive maintenance, cleaning the dust/dirt on these IGBTs and Diodes takes about 2 hours.

1.1.4. Direct contact single Phase Liquid Cooling

It is obvious that, for high power density equipment, air-cooled systems can't be the best solution in terms of efficiency and reliability. Liquid cooling is capable of supporting high density power and offer a wide range of advantages. Direct liquid cooling permits contact between liquid coolants and electronic component's Heat sink (Cold plate). Such type Direct contact liquid cooling can offer reduced thermal resistance and high heat exchange.

1.1.5. Structures of Liquid cooled Heat sinks

In liquid cooling of Heat Sinks, the basic heat sink structures based on flow channel are:

- Parallel channel type
- Pin fin type and
- Complex type

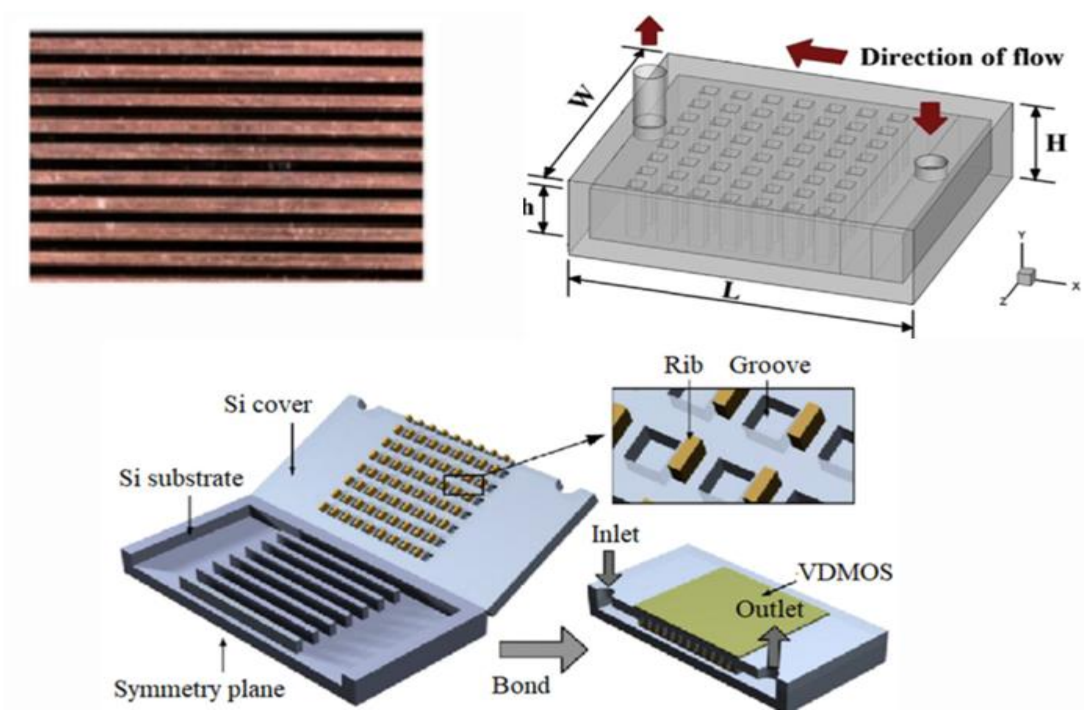

Figure 1.5. liquid cooled Heat sink structures

The parallel straight channel type heat sink has multiple straight channels arranged in parallel, with thin solid walls separating neighboring channels. Straight channels are advantageous as there is minimum pressure drop. Flow distribution is an influencing factor for the performance of this type heat sink. In pin fin type heat sink cooling, the liquid flow domain is a cavity filled with an array having the same height. The fin shapes can be rectangular, triangular, circular or some other. Complex hit sink structures may comprise a combination of cavity, rib, and parallel-straight channels or the use of porous medium.

1.1.6. Flow Distribution of Liquid cooled heat sinks

Non uniform fluid distribution to parallel channels decreases thermal performance of a heat sink and temperature hot spots may also be formed. To deliver coolants properly to flow channels, an optimization on distribution approaches is needed. The following are areas of optimization for efficient fluid flow distribution:

- Arrangement of heat sink inlet/outlet positions or injecting angle
- Design and structuraizon of the manifolds (headers); and
- Shape modification of the parallel channels.

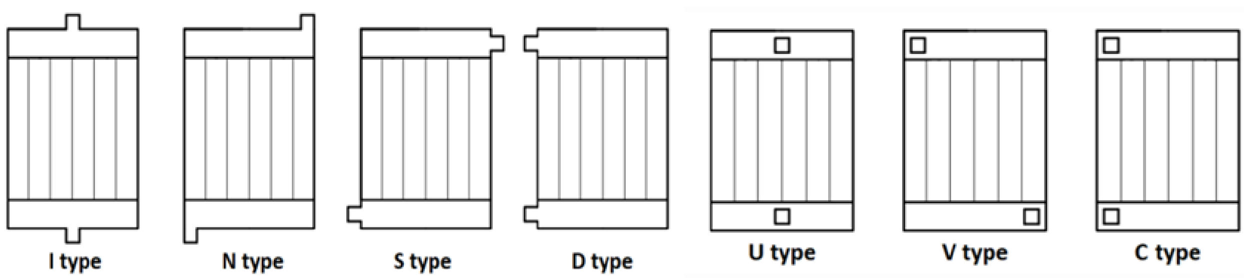

Figure 1.6. Coolant inlet outlet positions and manifold structure

For a number of IGBTs and Diodes arranged in a cabinet series flow channel can be adopted for better heat dissipation, uniform flow distribution and coolant saving. Pressure drop is however the drawback of this arrangement.

1.1.7. Cold End of the working fluid (Heat Exchanger)

To cool the working fluid after it flows out of the heat sink (hot area), Heat exchanger must be used whether it is in gas – liquid or liquid – liquid form. Direct contact heat exchange helps for fast heat exchange. Parallel and counter flow heat Exchangers are suitable for liquid - liquid Heat Exchangers, while cross flow Heat Exchangers are usually used for gas – liquid heat exchanger application.

In parallel flow heat exchanger types both hot and cold fluids enter the heat exchanger at the same end and move in the same direction. In counter flow, the hot and cold fluids enter the heat exchanger at opposite end and travels in opposite direction. Cross flow heat Exchangers are relatively compact in their construction. Hot and cold fluids flow perpendicular to each other. The two fluids might be mixed or unmixed during heat exchange.

The heat exchanger size is decided based on the inlet and outlet flow rate of the fluid, thermal resistance and amount of heat to transfer. Material selection and calculation of the mentioned parameters are important during design. Pump and other accessories of the system can be selected based up on the heat sink (evaporator) and Heat Exchanger size.

1.2. Statement of the problem

Forced air electrical cabinet cooling systems are the most widely used cooling systems with their own draw backs. Issues for air cooling include loud operating noise, decreased efficiency with ambient temperature rise, dust accumulation on the converter system coming from outside (with fresh air), system complication due to more components, high maintenance cost and high electric power consumption for operation.

In Adama I wind turbines 4KW centrifugal fans are used to deliver fresh and cold air to converter cabinets. These fans are designed to keep the cabinet temperature below 40^0C and the IGBT’s core temperature below 100^0C. It has been a common trend to experience a cabinet and its components masked with dust. This dust acts as an insulating blanket, preventing proper convection cooling and causing overheat.

The mentioned and other challenges related to converter air cooling were the motivation to look in to more reliable and efficient cooling mechanism. All those problems can be minimized if efficient liquid cooling is adopted for the converter system.

1.3. Research Hypothesis

Using single phase direct contact liquid cooling for Wind Turbine Electric power converter system (IGBTs and Diodes heat sink) gives improved thermal performance and good heat dissipation ability than forced air cooling

1.4. General Objective

The general objective of the proposed study was to design and numerically investigate the performance of single phase direct contact liquid cooling system for Electrical power converter system of Adama I wind power plant.

1.5. Specific Objective

The specific objective of the study was to:

- design liquid cooling system for IGBT and Diode heat sink,
- numerically study thermal effects of different working fluids as a coolant,
- select the suitable working fluid,
- select best coolant inlet velocity &
- Compare liquid based cooling of Converter system with the existing forced air cooling.

1.6. Significance of the study

This study is significant since it offers an optional and reliable solution for power converter system cooling problems. As the current Active cooling has maintenance and dust accumulation issues, the proposed liquid cooling system will highly contribute to minimize or eliminate them.

Direct contact liquid cooling can offer an efficient thermal management as it allows uniform heat dissipation by conduction. It can also minimize IGBTs and Diodes failure due to over temperature or in effective cooling. This system is dust free cooling approach that greatly helps the wellbeing of electronics on IGBTs and Diodes.

1.7. Limitation of the study

The work was limited to design and Numerically study the thermal performance of single phase direct contact liquid based cooling for IGBT and Diode Heat sinks. Analytical analysis and sizing of cold end heat exchanger and other components was also done based on design requirements.

1.8. Operational Definition

Five IGBT sets and one Diode set are layered vertically on a single Cabinet. There are a total of two Cabinets side by side. The Heat sink attached to the IPM is oriented at the tip (rear end) of the sets. Forced air was directed to hit this part (Heat sink) top to down and flows out of the cabinet in the existing Air cooling setup.

In the proposed design (liquid based cooling, the Heat sink's channel was modified to be rectangular channel by adding only a liquid guide cover on it. One Pump is used to deliver the coolant to each cabinets. The coolant carrying pipe (Header pipe) distributes this fluid to each IGBT & Diode Heat sinks via an inlet collector. The Inlet collector is a small extension that is used to receive a coolant from main (Header) pipe and directs it to each channel of the Heat sink. The Heat sink has a total of 21 rectangular shape narrow channels.

Temperature difference along the Heat sink governs the Heat transfer within it. As the Heat generating device (module) is attached to the top wall of the Heat sink, Heat is transmitted by conduction up to the fluid channel wall. At this stage heat from the hot body to cold fluid is exchanged by convection. The fluid will carry away the absorbed heat to reject it at condenser section.

The coolants coming out of the Heat sinks are collected and made to flow in Return pipe by Outlet collector. The collector has a small pipe on its end which is capable of delivering the designed flow rate. At the end of the Return pipe, a condenser Heat exchanger exists. The heat exchanger allows the hot fluid from the cabinets to attain its inlet Temperature by cooling it down. The cooled water will then be pumped back to heat sink for cooling purpose.

Every components of the converter system (5 IGBTs and 1 Diode in a single cabinet) have series coolant line interconnection and joined with the second cabinet return line to outside for cooling.

Figure 8 shows simple layout of the proposed system. Odd number IGBTs (IGBT number 1, 3, 5, 7 and 9 are placed at the second cabinet while even numbered IGBTs (IGBT number 2, 4, 8 and 10 are placed at the first cabinet.

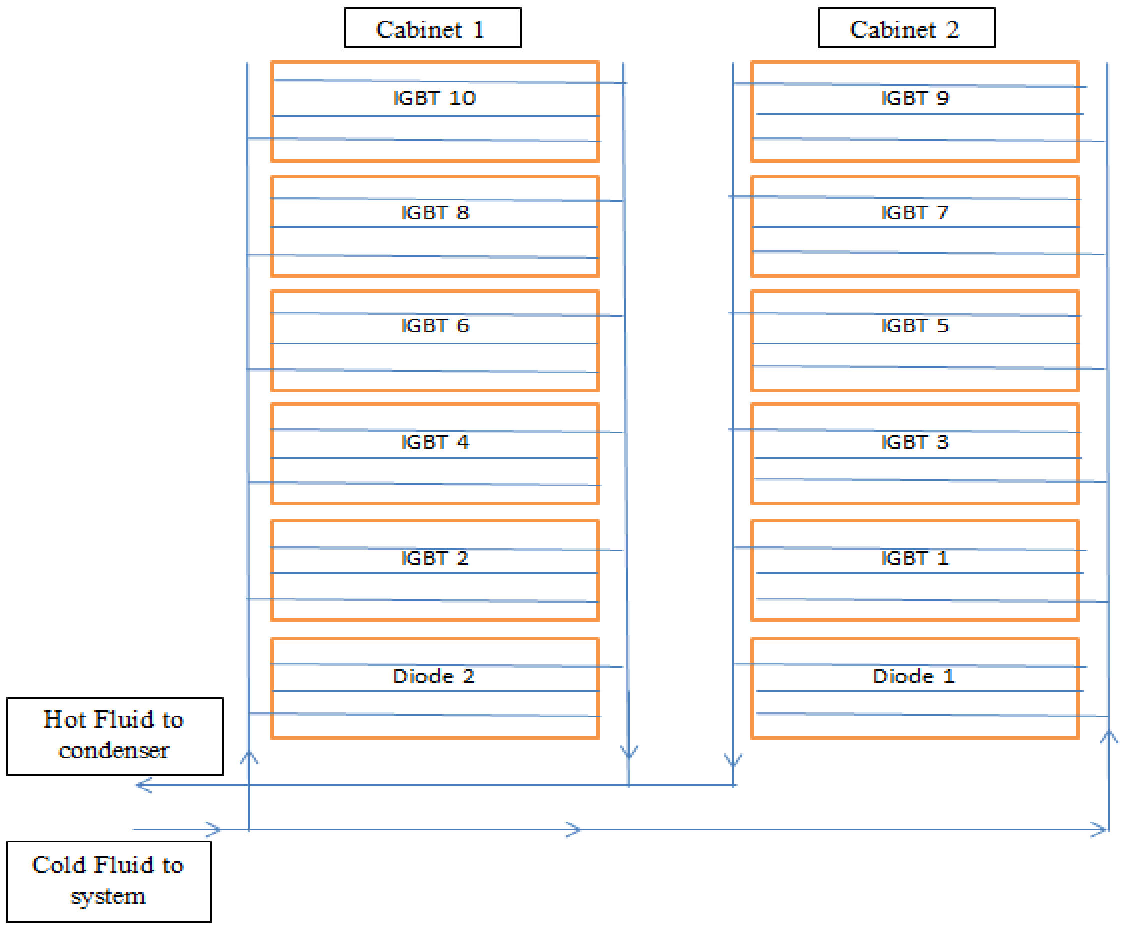

Figure 1.7. Proposed system layout

CHAPTER TWO

LITERATURE REVIEW

2.1. IGBT Cooling

Insulated gate bipolar transistors (IGBTs) are the main parts of wind turbine electric power Converter system. They normally losses much heat during operation. Cheng Qian et al. (2018), divided IGBT heat losses in to conduction losses and switching losses. The conduction losses occur during the on-state voltage drop across the IGBTs depending on the conducted current. Whereas the switching power losses occur during on and off stages of the IGBTs depending on the current, duty cycle, switching voltage and switching frequency.

If the heat generated by the IGBT modules cannot be eliminated efficiently, failure due to overheating will occur. The failure in converter system will in turn affect power production of the turbine.

Though liquid cooling has more complex construction than natural convective cooling via fins, forced air cooling and phase change cooling, it offers high thermal efficiency and compatible for high power devices.

Some IGBT heat sinks are designed to be cooled by air while high heat flow density IGBTs are structured as liquid cooled. Direct liquid cooling approach has high heat exchange efficiency as it uses conduction heat transfer. In such type of liquid cooling, A coolant is made to pass through the heat sink (lower plate of the IGBT) taking away the heat generated by the module.

2.2. Liquid cooled Heat sinks

According to Laloya et al. (2015), Heat sinks operate on conduction heat exchange mechanism. Most of the time heat sinks are made from aluminum. The thermal conductivity of aluminum is about 200 W/m. K and the maximum heat flux able to be dissipated depends on geometry.

Li et al. (2023) have evaluated the performance of series flow channel water-cooled plate for IGBT modules. They have studied the performance of three different series flow channel structures (namely conventional S-type, the double-helical type, and the Double-S-type flow channels) using computational fluid dynamics (CFD). The results show that the water-cooled plate with double-helical-type flow channel structure has the best comprehensive performance.

Channel width, channel height, and cold plate wall thickness and corner spacing of flow channel have been found to be an influencing factor for flow characteristics. The optimized design of the selected type cooling style resulted in reduced IGBT temperature, overall thermal resistance and pressure drop of the heat sink than that of double S-type structure.

Han et al. (2021) designed integrated liquid cooled heat sink for a 30kW motor inverter. For an optimum liquid cooled heat sink design, three arrangements namely, heat sink with the counter flow channel cooling, double U-shaped counter-flow channel, the serpentine channel configuration were analyzed. Neglecting natural convection and radiation, the analysis considered single phase (water), incompressible laminar and turbulent flow. Finally, the heat sink with serpentine channel configuration was selected due to its best temperature uniformity and cooling characteristic.

Li et al. (2017) studied the heat transfer performance water-cooled microchannel heat sink with dimple and pin-fin numerically. According to the research structure parameters such as pin fin diameter, dimple depth and stream wise spacing has effect on flow structure and heat transfer. The results show that the proposed designs exhibit heat transfer augmentation with energy saving and low-resistance features.

The relationship between the thermal-hydraulic performances and the layout of cooling channels, topology optimization was used by Li et al. (2019). Topology optimization (TO) can be used to develop the cooling channel layout automatically. The researchers focused on bringing a solution for flow distribution problem and heat exchange maximization problem.

Serpentine-shaped (S-shaped) cooling channel layout is employed and the cooling channel designed based on maximum heat exchange problem results minimum thermal resistance since it has the maximum area of fluid-solid boundaries. On the other hand, the cooling channel designed based on flow distribution problem can provide the minimum hydraulic resistance due to the optimization objective of Min. fluid power dissipation term. In general, this study revealed that, Topology optimization approach is effective to increase thermal and hydraulic performance of the coolant.

In the design of liquid IGBT module cooling, the selection of compatible cooling fluid is essential as it decides thermal efficiency of the cooling system and minimizes the risk of corrosion.

For aluminum heat sinks, glycol solution with dielectric fluids and oil are recommended as a working fluid. Water is also the best choice of liquid cooling as it has high heat capacity and thermal conductivity. When selecting water as a working fluid, attention on its mineral composition must be given since dosed presence of some minerals affect its conductivity and maximize water corrosion.

According to experimental work by Sprlak et al. (2014), direct liquid cooled heat sink's thermal resistance is affected by number of cooling ducts (contact surface), cooling medium capacity, stability of the fluid, temperature of the fluid. In their simulation, inlet temperature of the fluid to IGBT module was set at 300K. Three IGBTs were connected on the system and the maximum heat sink temperature from them was found to be 51.6^0C. Problem with this heat sink cooling was flow rate fluctuation of the fluid. The researchers concluded that this problem is caused by construction of heat sink.

In general, the water-cooled heat sink has higher thermal capacity than the air-cooled heat sink, but it needs additional equipment such as a heat exchanger, pump, and so on. Chang-Woo Han & Seung-Boong Jeong Predicted (calculated the Junction temperature of an IGBT module which is a key factor in thermal performance of the Equipment and for numerical evaluation. They used indirect measurement method to obtain this temperature.

An article review by Pan et al. (2021) states that hybrid solid and liquid cooling is a promising thermal management solution that can minimize more than 90% temperature non-uniformity on the IGBT. According to their study, direct liquid cooling using a micro channel cold plate can reduce thermal resistance and heat sink size of IGBT power module effectively. According to Liang et al. (2020), increasing the heat transfer surface area helps to reduce the convective thermal resistance. This shows that optimization in flow channel size is important. The higher the density and specific heat capacity of the coolant, the more heat can be carried by the unit volume of the fluid.

Han et al. (2016) compared heat transfer capabilities of conventional single-phase and two-phase cooling systems for electric vehicle IGBT power module. They finally concluded that two phase cooling has offers temperature distribution and higher temperature gradient. To achieve the phase change, vapor compression is the most appropriate system.

Taheri et al. (2020) studied to enhance the heat transfer performance of electrical modules a conventional heat sink heat pipe was modified by implementing an inlet and outlet in the heat sink to create a single continuous circulation path for the cooling fluid. Experiments were carried out to characterize the proposed cooling system in which the cooling fluid passes through the heat sink at different flow rates. The presented liquid-based heat sink with a new design was found as an appropriate candidate to overcome the weak cooling performance of the air-based heat sink.

The performance of direct contact liquid based electronic cooling will also depend on its cold end operating conditions, where the condenser is the key of the heat exchange system. According to Haldkar et al. (2013) cooling water temperature and flow rate have influence on the performance of condensers.

Lower flow rate results in an increase on condenser pressure than design value & poor heat transfer will occur. This pressure in the surface condenser will depend on condenser design, the amount of latent heat to be removed, cooling water temperature and flow rate, maintenance of the condenser and air removal system.

Silaipillayarputhur et al. (2019) stated that Log mean temperature difference (LMTD) and effectiveness-number of transfer units (ε-NTU) are analytical methods in the design of a heat exchanger (condenser). exchanger. ε-NTU is more flexible as it can be used when the fluid discharge temperatures are unknown. But both LMTD and ε-NTU techniques yield the same exact results.

Unuvarn et al. (2004) considered two variable categories in heat exchanger design. These include process design and mechanical design. Working fluid type, flow rates and amount of fluid entrance and exit temperature, amount of vaporization or condensation, operating pressures and allowable pressure drops, fouling factors, and rate of heat transfer are process variables. Mechanical information includes size of tubes, tube layout and pitch, maximum and minimum temperatures and pressures, necessary corrosion allowances, special codes involved, recommended materials of construction.

Ayhan Nazmi and Ahmet Yayli (2022) studied the performance of different cold plates with different geometry to maintain the thermal stability of li-ion battery. keeping the outer dimensions constant and variable flow, series, parallel, series-parallel arrangements were studied numerically for the effect on thermal resistance and pressure drop. Series-Parallel arrangement was finally found for best Heat transfer and minimum pressure drop.

Xiang Peng et al. simulated multi-stream plate fin heat exchanger based on integral mean temperature difference method. Hybid particle swarm algorizm was used to design space for different operating conditions.

Jyoti Pandey et al. (2014) Compared parallel and pin fin channel cold plates with water as coolant. The power to deliver the fluid was found in parallel channel at the same Reynolds number. Thermal resistance was able to drop by 27.7% by increasing pin fin length. The study investigated that pin fin arrangement results in high power loss.

To obtain sufficient amount of flow and good fluid distribution for electronics cooling, Kanchan M. et al. used Flow Network Modeling (FNM). This technique uses overall flow and thermal behaviour to predict components size.

Satish G et al. (2012) Prepared Design considerations during the design of high power device liquid cooling. According to them Heat transfer from IGBT to its Heat sink can be maximized by using ceramics with high thermal conductivity, internal fins in liquid passages, using micro channels.

Georgios Mademlis et al. (2021) designed heatsink geometries for three-phase SiC inverters comparing their thermal performance in terms of pressure drop of the coolant and attained temperatures of the inverter power modules. A number of heat sink geometries like wavy shaped fins, straight cooling channels and rectangular pin shaped fins were developed to attain uniform temperature distribution at the surface of the heat sink.
Thermal simulations have shown that the heat sink with rectangular pins can be tuned through an iterative design process to alleviate the thermal gradient at the surface of the sink by carefully placing the pins and dividing the coolant flow evenly to the three power modules. The average temperatures of the three power modules differ less than 2^0C in the final heat sink design, while the three power module temperatures can differ more than 16^0C in the previous wavy-fin designs. The highest temperature at the surface of the final heat sink is also 90oC, while the coolant experiences a pressure drop of 16 mbar for flow rates of 10 l/min. The attained even thermal

distribution of the heat sink allows equal aging of the power modules, thus increasing the total lifetime of the system.

Different channel shapes have different heat dissipation performance. For example, circular pipe has small flow resistance than other shapes with the same cross sectional area.

2.3. Research gaps

The first gap observed in the Literatures was, non-uniform temperature distribution on the heat sinks (target bodies). This is mostly caused by poor flow channel design and construction (Pan et al., 2021). The conventional heat sink flow channels (bend tube integrated on the heat sink) result temperature non uniformity throughout the object.

Type of flow construction also influences flow fluctuation which in turn leads to temperature non-uniformity (Sprlak et al. 2014). Water mineral composition was not dealt properly on the reviewed researches. Using water as a liquid coolant without knowing its ingredients leads to poor cooling effect, corrosion effect, biological fouling and scaling.

Some of the researchers use two phase passive cooling. This approach needs complex system setup. In this system, air is used to dissipate heat from cold end. The heat exchange between the solid materials and air is mainly depended on the contact area.

For the case that the heat spreading area to exchange and dissipate heat is small, there will be a bottleneck between the terminal heat sink and the ambient. Therefore, no such a complex solution will help to avoid the use of active cooling in this case (Cheng Qian et al., 2018)

Table 2.1. Summary of literature review

Article	Heat Ex influencing parameters	Result	Research gap
[4] Performance Evaluation and Optimization of Series Flow Channel Water Cooled Plate for IGBT Modules (Liyi He et al., 2023)	Channel width, height, plate thickness & corner spacing	Double helical type flow channel shows reduced IGBT T^0, Thermal resistance and pressure drop	
[2] Design and optimization of a liquid cooled heat sink for a motor inverter in electric vehicles (Feng Han et al. 2021)	Fin thickness, fluid flow	Heat sink with serpentine channel configuration was selected due to its best temperature uniformity and cooling characteristic.	Effect of cold liquid inlet temperature was not studied
[3] Experimental and numerical investigation of liquid-cooled heat sinks designed by topology optimization (Hao Li, 2019)		flow distribution design can provide the lowest hydraulic resistance while the heat exchange maximization design can keep the thermal resistance to a minimum.	Flow channel geometry influence on the system was not studied
[6] Design of Experimental Liquid Heat sink for High Power Electronic (Roman et al. 2014)	Fluid flow rate	It was able to keep the temperature of three IGBTs connected on the system below 52^0C.	Degradation of flow rate was not able to control due to heat sink construction

[1] Evaluation of the thermal performance with different fin shapes of the air-cooled heat sink for power electronic applications (Chang-Woo Han & Seung-Boong Jeong, 2016)	Heat sink shape and type	junction temperature of the IGBT module was predicted	Couldn't show the effect of fin size (thickness, length etc..)
[7] An Energy Analysis of Condenser (Vikram et al. 2013)	Fluid temperature & flow rate	pressure on condenser depend latent heat to be removed, cooling water temperature and flow rate	-

Based on the reviewed Literatures, the following points were drawn:

Table 1.2. Concluding points from Literature review

Suitable Heat sink structure	• Parallel flow channel heat sink structure
Most widely used working fluids	• Water • Mixture of Water and Glycol • Oil
Flow influencing factors	• Coolant I/O arrangement • Coolant inlet T • Fluid flow rate • Flow channel size & geometry

CHAPTER THREE

MATERIALS AND METHODS

3.1. Data Collection

The necessary information for the research work was collected from different available sources. These include Name plates, User manuals, Maintenance manuals, SCADA, Actual measurement, Data sheets and Books.

3.1.1. Name Plates

Name plates outline necessary information about the type, model, rating, manufacturer name and serial number of a certain machine. Some information about Power converter (IGBTs), Cooling fans and so on were obtained from their tag or name plate.

3.1.2. Maintenance manuals & User manuals

These manuals offer detail behavior of the devices and maintenance approaches to follow. Constructional and operational elaboration of the converter system was found inside the manufacturer and installer manuals. Thermal management of this system and its cabinet was found in SEMIKRON user manual and Goldwind Wind turbines maintenance and operation manual.

3.1.3. SCADA

Supervisory Control and Data Acquisition (SCADA) system is used for controlling, monitoring, and analyzing wind farm turbines and other facilities. The system consists of both software and hardware components and enables remote and on-site gathering of data from the farm. The wind turbines live status and fault history is also recorded on this system.

3.1.3. Actual measurement

To know dimension and some other electrical physical quantities, actual measurement is mandatory. Sound meter, Tape meter, caliper, Thermometer and digital multi meter are among the instruments used.

3.2. Article reviews, Data sheets and Books

These are the main information sources for the research work as they offer previous experimental and numerical works, scientific facts, standards and reference materials.

3.3. Data Analysis

After gathering important data for the research work, it was interpreted, organized and analyzed to get a meaningful result. Some simple problems may require analytical analysis while complicated problems require numerical computation using software.

3.3.1. Mathematical Modeling

Mathematical equations were developed as needed to represent the behavior and characteristics of the system under study or its process. This formed basis for numerical modeling and simulation. So as to determine the size and heat transfer rate of the proposed system analytically, assumptions were made.

Different governing equations were used based on predefined assumptions to calculate the performance and behavior indicator entities.

3.3.2. Geometry Design

The optimized model(s) was designed on ANSYS Design Modeler and Space claim softwares based on calculated dimensions. The Geometry was modeled using the same dimension as that of the actual object. The top center wall of the Heat sink was made by split face principle for easy application of heat flux on it. No change was made on the number of the flow channels as the purpose of the work is to improve the cooling system using original geometry.

3.3.3. Numerical Simulation

The proposed model was subjected for a given computerized thermal system to various inputs, such as operating conditions, to determine how it behaves and thus predict the characteristics of the actual physical system. This approach can represent the real system and can estimate the accuracy of numerical algorithm.

For numerical simulation, CFD software called ANSYS FLUENT will be used to model the characteristics of heat transfer of the system. This software uses a finite volume method to solve the governing equations of fluid flow and heat transfer.

Geometry Insertion: Geometry of the model was inserted from other sources

Meshing: For better result of the simulation, the geometry must be processed separately by breaking it in to small parts. The finer the mesh is, the better the results.

Setting up and obtaining solution: At this stage, boundary conditions, grid independence test, calculation for result and result generation was done.

3.3.4. Validation work

After obtaining Simulation Result, it was compared with the existing system (Air cooled) thermal performance.

3.4. Document Compilation and Submission

The final stage of the work was to prepare the research document. In this stage, the previously collected data, Simulation results, Article reviews and other theoretical ideas were organized and documented in a reader friendly way.

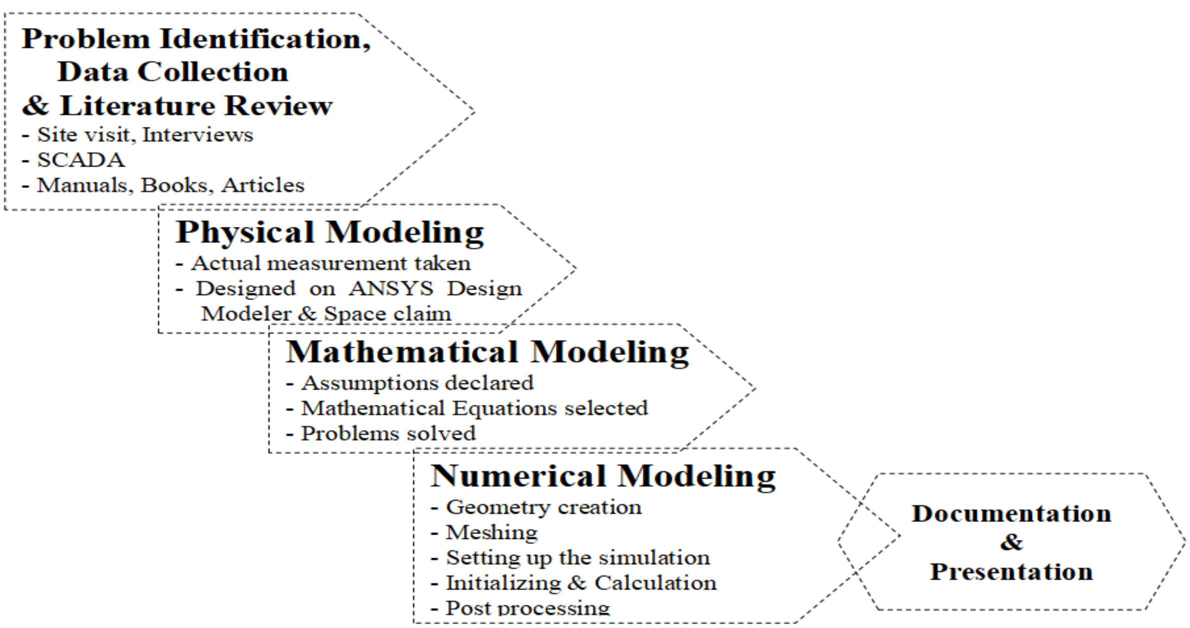

Figure 3.1. Overall work Methodology

CHAPTER FOUR

DESIGN OF THE SYSTEM AND NUMERICAL MODELING

4.1. General

The converter System is grouped in to two cabinets. Each cabinet encloses 5 IGBT sets and 1 Diode. This study considers the system setup only by adding piping system, Heat Exchanger and Pump. A fluid collector allows the exist coolant to return pipe and directs inlet coolant to the Heat sink.

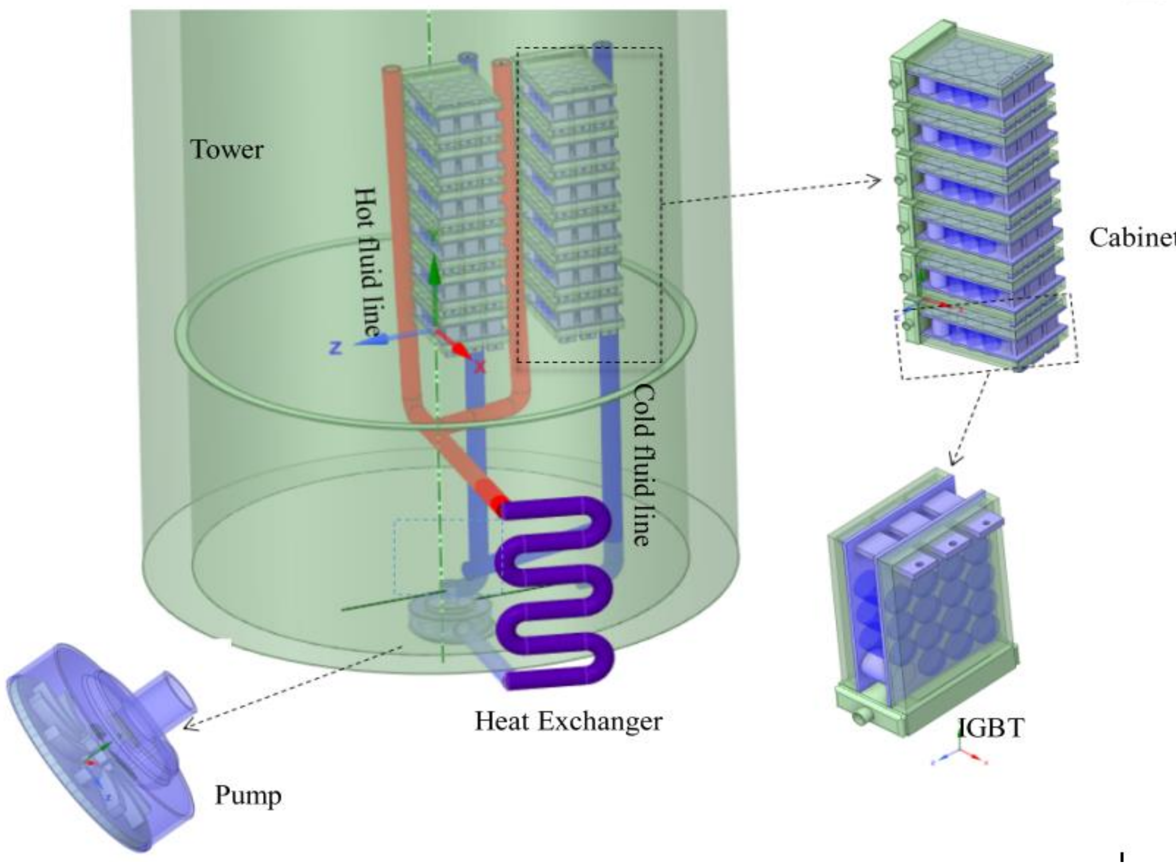

Figure 4.1. Complete system Setup of the Liquid based Converter cooling

To predict the detail heat transfer and fluid flow behavior of the Heat sink, Computational fluid dynamics approach is used. Its solution is solved numerically based on Governing equations such as equations of continuity, conservation of momentum, and conservation of energy for different flow regimes. Other components sizing and analysis is performed analytically.

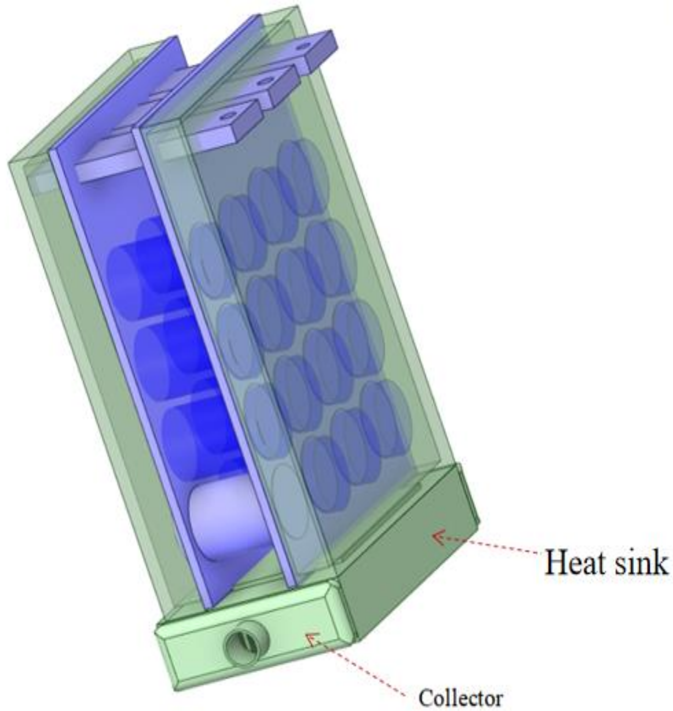

Figure 4.2. IGBT/DIODE set with collector

4.2. Fluid flow type

It is important to know the flow type to predict and control fluid behavior. When fluid flows without disturbance in parallel layers it is said Laminar flow. In this case the flow pattern is smooth. On the other hand, fluid mixing occurs when there is irregular flow of fluid particles. This type of flow with higher resistance and unpredictable behavior is categorized as Turbulent flow.

To determine the type of flow pattern as laminar or turbulent, a dimensionless parameter called Reynolds number is used. It is the ratio of inertial forces to that of viscous forces. Low Reynolds number ($Re < 2000$) indicates Laminar flow while higher Reynolds number ($Re > 4000$) represents turbulent flow. In between these two distinctions, Transitional state from laminar to turbulent flow is represented.

The following section presents calculation for Reynolds number at different flow inlet velocities. Three coolant (fluid) inlet velocities were selected for optimization. As fluid velocity is directly related to flow rate, the effect of flow rate on cooling the heat sink was studied.

Reynolds number depends on fluid's density, velocity, viscosity and flow channel hydraulic diameter. Hydraulic Diameter is a characteristic dimension for internal flow situations in shapes such as squares, rectangular or annular ducts where the height and width are comparable. It can be calculated by the cross-sectional area and the wetted perimeter of the ducts.

For Rectangular Channels, Hydraulic diameter can be calculated as

$$D_h = \frac{4A}{P} = \frac{4(wh)}{2(w+h)} = \frac{2\,(wh)}{w+h} = \frac{2\,(0.005 \text{ x } 0.05)\text{m2}}{(0.005+0.05)\text{m}} = 0.0091\text{m}$$

$$R_e = \frac{\rho VDh}{\mu} \qquad \text{For v = 0.4m/s} \qquad R_e = \frac{998.2 \text{ x } 0.4 \text{ x } 0.0091}{0.001003} = 3623$$

$$\text{For v = 0.6m/s} \qquad R_e = \frac{998.2 \text{ x } 0.6\text{x } 0.0091}{0.001003} = 5434$$

$$\text{For v = 0.8m/s} \qquad R_e = \frac{998.2 \text{ x } 0.8 \text{ x } 0.0091}{0.001003} = 7245$$

Where D_h = hydraulic diameter (in m)

A = Flow channel Area

P =Wetted Perimeter

w = width of the channel

h = height of the duct

From the given inlet fluid velocity and flow area the inlet Volume flow rate (V) is the amount of fluid that passes through a predetermined flow area per unit of time. The maximum allowable flow rate allowed for liquid heat sink cooling is given as $0.0002\text{m}^3/\text{s}$ by the manufacturer. So that flow rates less than this are taken for Analysis.

$$V = v\,(w\ x\ h) \qquad \text{For v = 0.4m/s} \qquad V\ = 0.4\,(0.005\ x\ 0.05) = 0.0001\text{m}^3/\text{s}$$

$$\text{For v = 0.6m/s} \qquad V = 0.6(0.005\ x\ 0.05) = 0.00015\text{m}^3/\text{s}$$

$$\text{For v = 0.8m/s} \qquad V = 0.8\,(0.005\ x\ 0.05) = 0.0002\text{m}^3/\text{s}$$

4.3. Mathematical Modeling

Mathematical equations are developed to represent the behavior of the physical system under study. This will form basis for numerical modeling and simulation. So as to predict the fluid flow and heat transfer characteristics of the system, the following generalized assumptions were made.

- The fluid is Newtonian and Incompressible
- There is no internal heat generation from the fluid
- There is no phase change in the fluid flow
- The operation is steady state operation
- There is no radiation effect
- The effect of gravity is neglected

Based on these predefined assumptions Governing equations were formulated.

4.3.1. Conservation of Mass (Continuity Equation)

$$\frac{\partial u}{\partial x} + \frac{\partial v}{\partial y} + \frac{\partial w}{\partial z} = 0$$

where u, v, and w are the velocity components of the fluid velocity in the x, y, and z directions.

4.3.2. Conservation of Momentum

Conservation of linear momentum is also known as the Navier-Stokes equation. Navier-Stokes is usually used to include both momentum and continuity equations and even energy equation sometimes. It can be represented as:

$$\rho\ (\partial u/\partial t + u\ \partial u/\partial x + v\ \partial u/\partial x + w\ \partial u/\partial x) = -\partial P/\partial x + \mu\ (\partial^2 u/\partial x^2 + \partial^2 u\ /\partial y^2 + \partial^2 u\ /\partial z^2)$$

$$\rho\ (\partial v/\partial t + u\ \partial v/\partial x + v\ \partial v/\partial x + w\ \partial v/\partial x) = -\partial P/\partial y + \mu\ (\partial^2 v\ /\partial x^2 + \partial^2 v\ /\partial y^2 + \partial^2 v/\partial z^2)$$

$$\rho\ (\partial w/\partial t + u\ \partial w/\partial x + v\ \partial w/\partial x + w\ \partial w/\partial x) = -\partial P/\partial z + \mu\ (\partial^2 w/\partial x^2 + \partial^2 w\ /\partial y^2 + \partial^2 w\ /\partial z^2)$$

where ρ is the fluid density, P is the pressure, and μ is the dynamic viscosity of the fluid.

4.3.3. Energy Equation

$$\rho\ C_p(\partial T/\partial t + u\ \partial T/\partial x + v\ \partial T/\partial x + w\ \partial T/\partial x) = k\ (\partial^2 T/\partial x^2 + \partial^2 T/\partial y^2 + \partial^2 T/\partial z^2)$$

where Cp is the specific heat capacity, T is the temperature, and k is the thermal conductivity of the fluid. This energy equation is derived by considering the conduction heat transfer governed by Fourier's law with being the thermal conductivity of the fluid.

4.3.3. Heat Transfer along the Solid (Heat Sink)

The heat transfer mode with in the solid Heat sink (from the top end up to bottom end) is heat conduction. Conduction heat transfer occurs from hotter end to colder end of solid object. The heat flow equation is as follows:

$$Q = KA\frac{T1-T2}{X}$$

where Q is transferred heat in the heat conduction process, T_1 and T_2 is the temperature at two points, k is the thermal conductivity thickness, x is thermal conductivity coefficient, and A is the thermal conductivity area.

4.3.4. Heat Transfer between the Heat sink and coolant

The heat transfer between the Heat sink and the coolant belongs to convective heat transfer, It can be represented as thermal convection model and its heat flow equation is as follows:

$$Q = hA\,(T_c - T_f)$$

where Q is heat transfer, T_c is the adjacent Heat sink wall Temperature, T_f is the coolant temperature, h is the convective heat transfer coefficient, and A is the heat transfer area.

4.4. Numerical Modeling

Numerical Modeling is used to obtain quantitative results of the system behavior for different operating conditions and design parameters. It is based on mathematical models. The Governing equations are solved computationally after discretization and restructuring them.

The following Numerical procedures were used to solve the mathematical model and predict the characteristics of the fluid and the solid.

- Geometry creation,
- Mesh creation,
- Grid independence tests,
- Preprocess and application of boundary conditions,
- Solution process and post-process phases.

ANSYS fluent was used to observe flow and heat transfer behavior of different flow regimes and solid surface. The software was used as tool for the numerical solution.

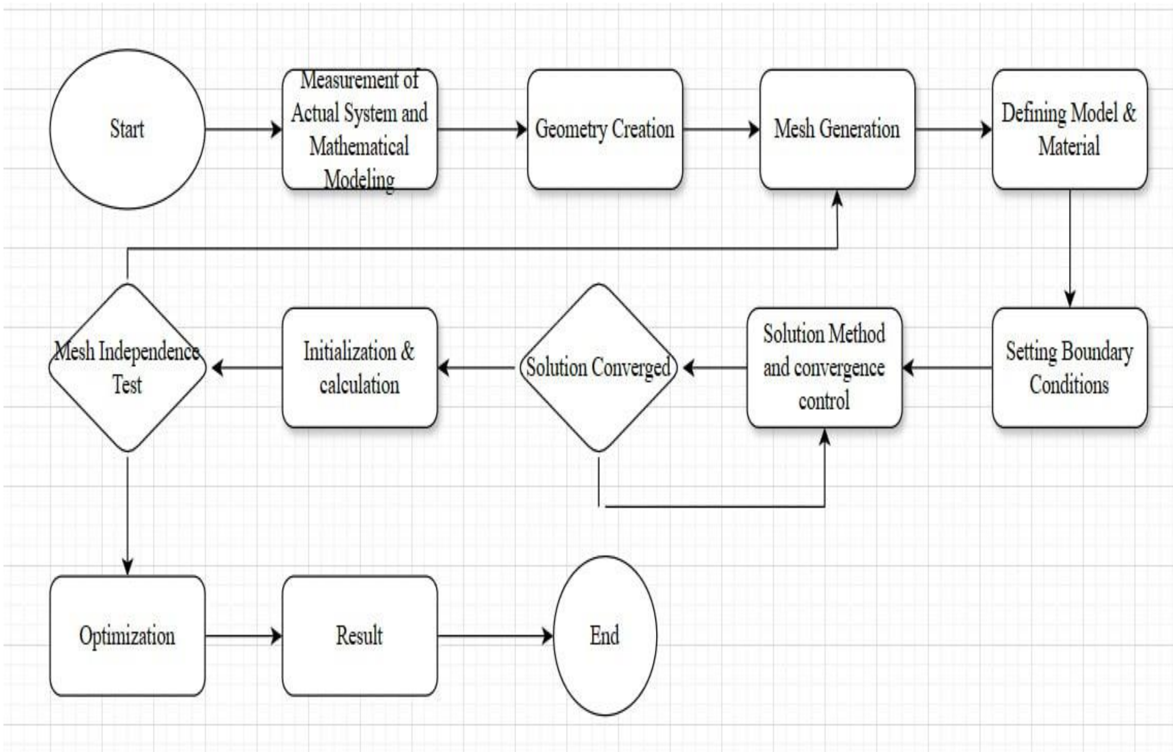

Figure 3.2. Numerical Work Procedure

4.4.1. Geometry Creation

The first step in numerical modeling is to create the geometry of the actual system. Heat sink with 21 fluid channels will be modeled for computation. A 3D geometry of the Heat sink was created by ANSYS Design modeler. Along with each channel of the Heat sink a rectangular fluid domain was formed by Boolean operation.

The Heat sink has an overall dimension of 0.36 x 0.215 x 0.07 m (L x W x H). Rectangular channels of 0.005 x 0.05 x 0.205 m (w x h x L) dimension with 0.05m wall thickness were formed to guide the fluid flow. The surface in which the IGBT module (heat source) is attached to the Heat sink is distinguished by Face split.

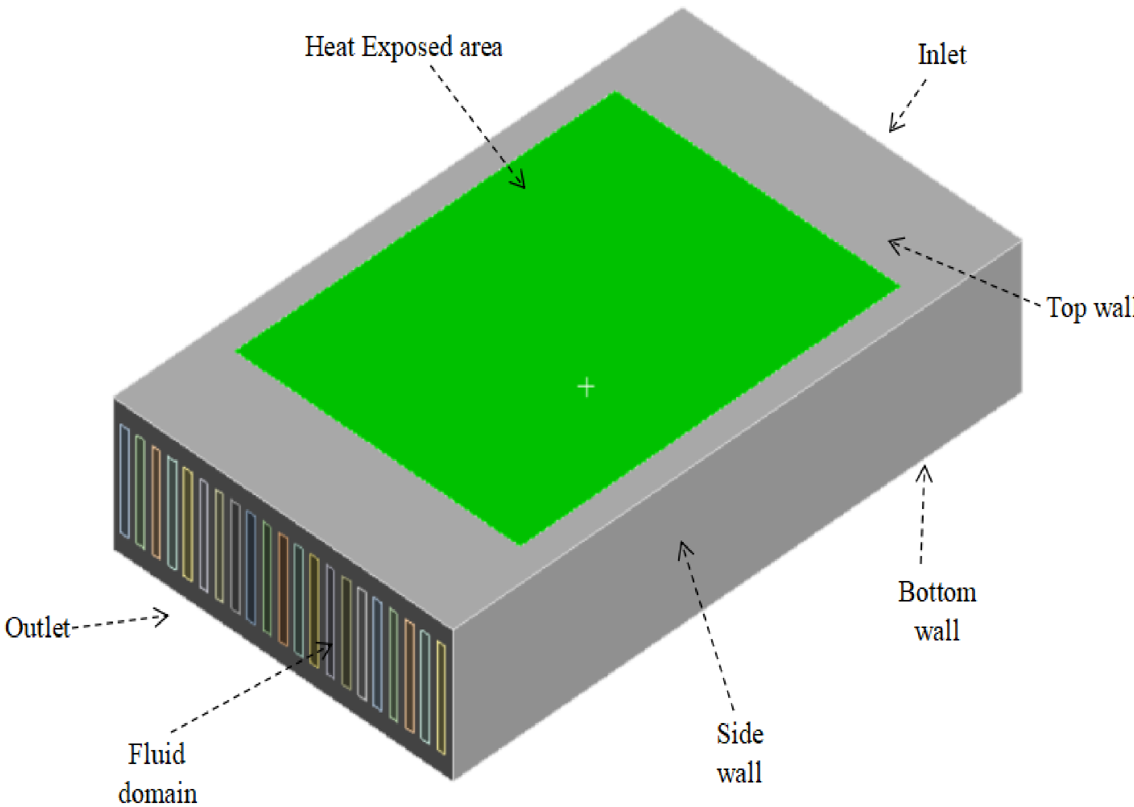

Figure 4.3. Geometry of the Heat sink

Since the aim of the work was only to change the air cooled heat sink to liquid cooled, no change on size of the existing heat sink was made. There are 4 Power modules which are attached at the heat exposed surface of the Heat sink. Their total surface area can't exceed this area.

4.4.2. Meshing

Meshing is used to create computational grid. It is the process of discretizing a geometry surface or volume into multiple elements. These elements are used to calculate the required variables across the mesh using partial differential equations.

The mesh was generated for both the solid and the fluid Geometry by Body Sizing approach. An element size of 1.25mm (fluid domain) and 4mm (solid material) was selected after Grid Independence test.

Figure 4.4. Mesh display of the geometry

4.4.3. Grid Independence test

The number of tetrahedral elements was increased to obtain similar simulation results. This independent work is called Grid Independence test which is performed to check whether the simulation process and result is independent of the element size.

The variation of heat sink Temperature in function of the total number of Heat sink mesh elements is shown below. The Element size of fluid domain was kept constant (1.25mm) while that of Heat sink is increased from 2mm to 10mm. Maximum Temperature of Heat Sink and fluid didn't change that much after the 4^{th} mesh size.

This indicates that continuing to make the mesh finer will not change the result. Mesh size of 4mm is selected to decrease computational time. Water at 0.8m/s was used as a coolant fluid for the grid independence test.

Table 4.1. Variation of Heat sink average top surface Temperature with Mesh size

Mesh	Element size	Number of Elements	Number of Nodes	Heat sink Top surface Temperature (°C)
Mesh 1	10 mm	991391	1226225	44
Mesh 2	5 mm	1238008	5147103	46.625
Mesh 3	4 mm	1483006	1363211	47.88
Mesh 4	2.5 mm	2961506	7722382	47.8826
Mesh 5	2 mm	4737269	10256787	47.889

The number of Meshed elements versus Heat sink temperature is shown below.

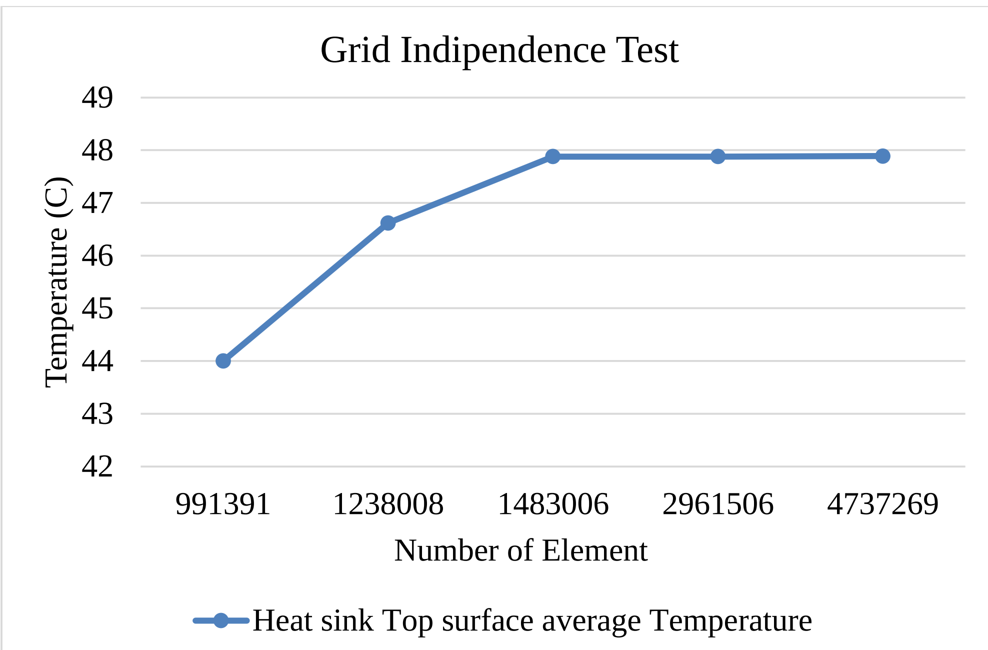

Figure 4.5. Grid Independence test

4.4.4. Numerical simulation setup

The fluid flow and the heat transfers were set to be steady state and solved by pressure based solver. The Numerical simulation was performed in 3D geometry model and steady state condition using ANSYS fluent.

4.4.5. Numerical Model

Energy Equation is enabled as the simulation contains heat transfer in addition to fluid flow. K - Omega was used in combination with SST.

4.4.6. Materials

Three fluid materials namely pure water, Glycol water mixture and mineral oil were studied whether they can achieve the desired cooling effect or not.

a. Purified water

Purified water is chemical and contaminant free liquid with operating temperature range of 0°C to 100°C. As an advantage, it has a superior heat transfer capacity compared to other fluids. In addition to this, it is nontoxic, easy to work or dispose, widely available and low cost. However, corrosion can be an issue if minerals and water are present in it.

The quality of water depends on its storage, delivery, and source (ground. It may contain corrosive impurities, such as chloride, alkaline carbonate salts, or suspended solids. Impure water is also an electrolytic bridge to enable galvanic corrosion if the system possesses dissimilar metals.

b. Glycol-water mixture

In order to lower the freezing point of water and increase its boiling point, glycols are used as an additive in water. These solutions can be used in both cold and hot environments with an operating Temperature range of 50°C to 150°C. Ethylene glycol and propylene glycol are the two most used glycols in these mixtures.

According to the desired heat transfer capacity and freeze protection, the concentration of glycol can be varied. Higher concentrations of glycol provide better freeze protection but reduce the heat transfer efficiency of the mixture. Also guidelines and safety regulations must be followed to dispose glycol water mixtures as they have potential of toxicity.

c. Synthetic Mineral Oils

Mineral oil cooling is odorless, non-toxic and offers significant noise reduction compared to other liquid or air cooling systems. These oils have an operating temperature range of -40°C to 290°C. This make it ideal for using it where temperature at the heat source exceeds the operational temperature limit of water based coolants.

The solid (Heat Sink) and fluid materials with their respective thermal properties are summarized in the following table.

Table 4.2. Solid and Fluid materials with their properties

Part	Material	Chemical Formula	Density (kg/m3)	Thermal conductivity (w/m.k)	Specific heat J/(kg.k))	Viscosity (Kg/m s)
Solid	Aluminum	Al	2719	202.4	871	-
Fluid	Water	H_2O	998.2	0.6	4182	0.001003
	Glycol Water Mixture (0.5 conc.)	$C_2H_8O_3$	1076	0.47	3488.5	0.0017
	Mineral Oil	-	870	0.136	1900	0.002

4.4.7. Cell zones and Boundary conditions

a. Cell Zones

There were two cell zones that represent the volume of the fluid passing along the rectangular channels of the cold plate channel and the Aluminum cold plate itself. The materials used for the fluid are purified water, Glycol mixture and Mineral Oil.

b. Boundary Conditions

At the Inlet of the channel, Velocity inlet boundary condition was applied to define the flow velocity. Heat flux is applied to the face in which the Module is attached at the top wall.

Table 4.3. Boundary conditions of the system

Boundary	Condition	Values
Inlet	Velocity inlet	V_{in} = 0.4m/s, 0.6m/s, 0.8m/s
Outlet	Pressure outlet	$P_{gage} = 0$
Heat surface (Surface exposed to heat generating Module)	Heat flux	q” = 300000W/m^2
Heat sink Top, Bottom and Side walls	Adiabatic	-
Fluid-solid interface	Conjugate heat transfer	Coupled wall
Other walls	Adiabatic	-

4.4.8. Solution Methods, Initialization and Calculation

SIMPLE solution scheme with Green-Gauss cell based gradient was used in the calculation. For better convergence First order discretization was selected.

The computational fluid dynamics is completed if the solution is converged. Residual monitoring is used to check the convergence of the solution. 10^{-3} was set as an absolute criterion to all equations (continuity, X-velocity, Y-velocity, Z-velocity, Energy, K and Omega). After initializing the solution from inlet, the calculation was made to run by setting 1000 Iterations to store.

CHAPTER FIVE

RESULTS AND DISCUSSIONS

5.1. Numerical Study of Heat Sink Thermal Property with different liquids

5.1.1. Average Heat Sink Temperature

The main purpose of this study was to maintain the thermal stability of the Heat sink. This depends on the heat applied, thermal conductivity of its material and fluid inlet temperature. At the same fluid inlet velocity and input parameters, the three fluids showed different cooling effect on the Heat sink.

As it was discussed in the previous chapter, 30w/cm^2 heat flux was applied to the top wall of the heat sink. This heat transferred through the heat sink by conduction and energy exchange will occur with the cold fluid at each flow channels. The inlet temperature of the fluids was kept as 25^{0}C.

Using water as a coolant resulted in best cooling effect. The maximum average Heat sink temperature (top surface) at 0.8m/s fluid inlet velocity was 47.88^{0}C. Glycol water mixture with 50% mass concentration cools the Heat sink up to 51.4^{0}C. Mineral Oil had the least cooling performance (can lower the heat sink Temperature up to the minimum of 97.86^{0}C which is higher).

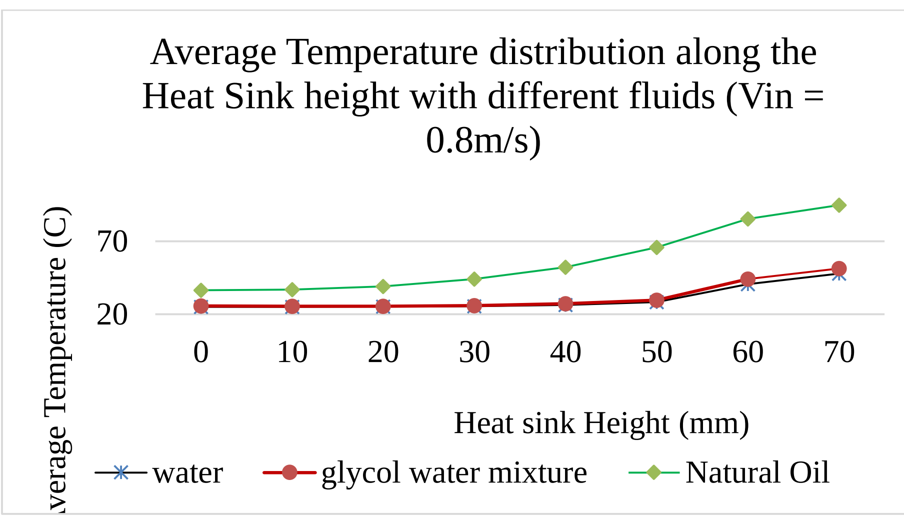

Figure 5.1. Average Temperature distribution along the Heat Sink height with different fluids (at Vin = 0.8m/s)

Decreasing velocity of fluid decreases the mixing and circulation of the fluid. In result, Heat transfer between the fluid and the solid body decreases. This was what happened on Converter system Heat sink cooling. As the fluids velocity was lowered to 0.6m/s and 0.4m/s, their cooling effect was lowered consequently.

Pure water, Glycol water mixture and Natural Oil decreased the top surface of the Heat sink up to 49.74^0C , 71.94^0C and 73.8^0C respectively at 0.6m/s inlet velocity.

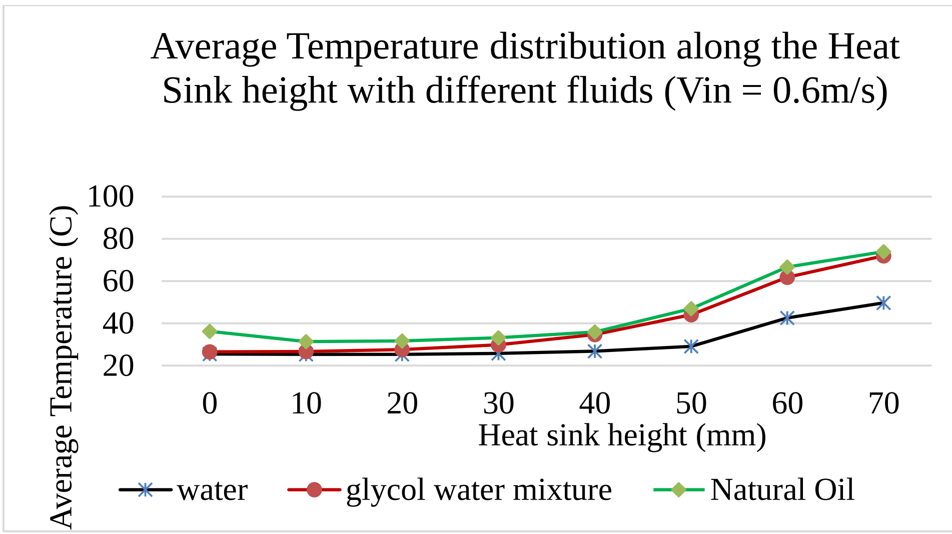

Figure 5.2. Average Temperature distribution along the Heat Sink height with different fluids (at Vin = 0.6m/s)

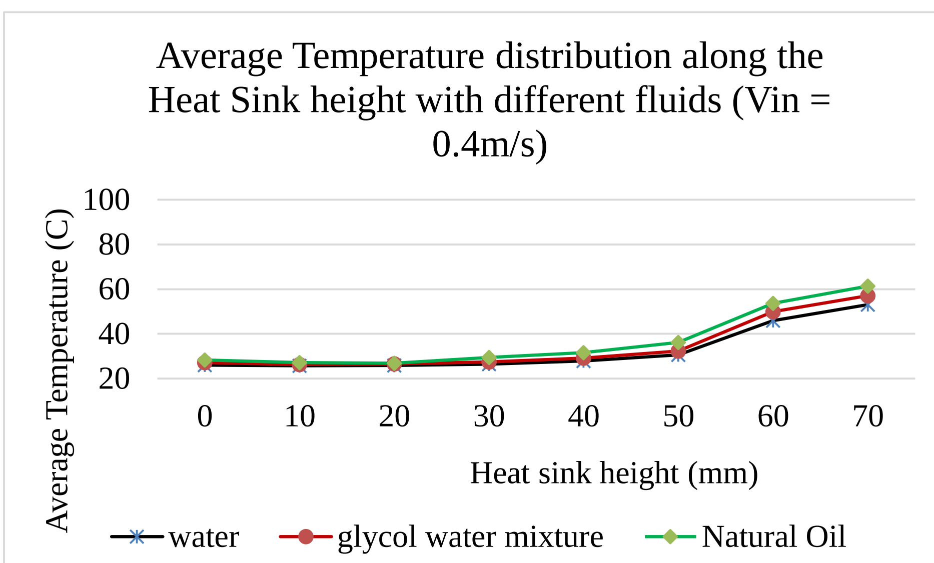

Figure 5.3. Average Temperature distribution along the Heat Sink height with different fluids (at Vin = 0.4m/s)

The effect of flow velocity continues to decrease the cooling performance. At 0.4m/s flow velocity, maximum top wall Temperature of 53.13^{0}C, 57.11^{0}C and 61.32^{0}C was obtained for pure water, Glycol water and Oil respectively.

5.1.2. Heat sink average Temperature distribution along fluid flow direction

The Temperature of the Heat sink varies along its distance. As the heat exposed surface is at the mid, it's Temperature rises up to the 60's mm and stays nearly constant for the next 240mms. After this point it will decline up to the fluids outlet Temperature. The heat generating parts of the IGBT or DIODE set are the power modules attached at the mid top of their heat sink. The rest area of the heat sink top surface is used as heat dissipation.

Still the temperature plot of Heat sink cooled by pure water showed minimum result which made it best choice to use it as coolant.

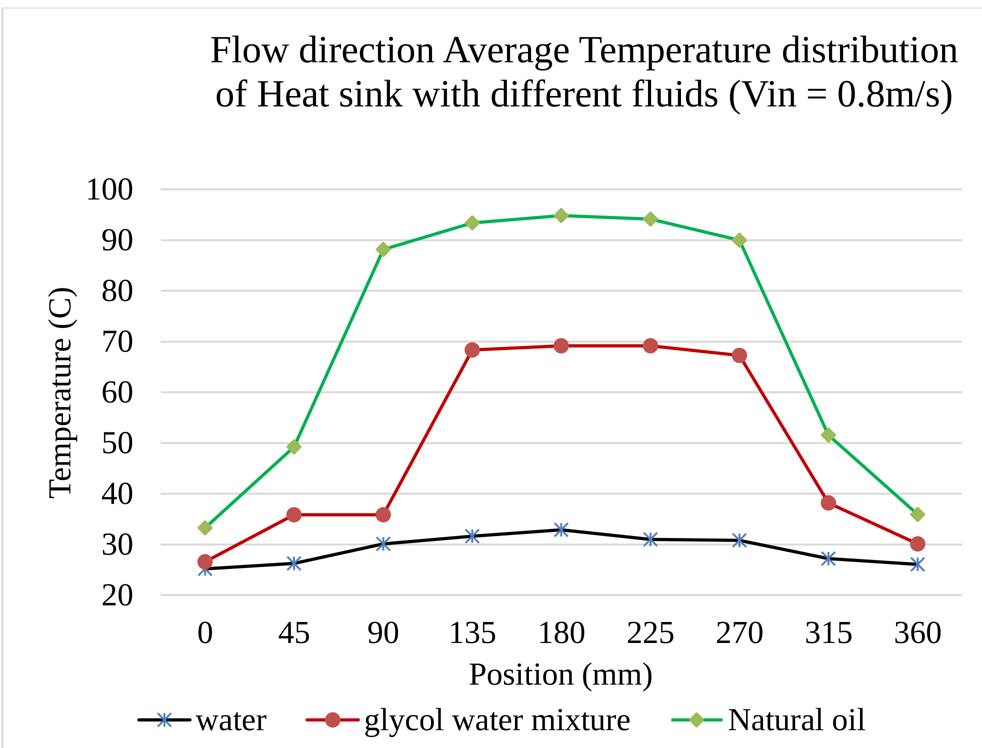

Figure 5.4. Flow Direction Heat sink Average Temperature comparison at Vin = 0.8m/s

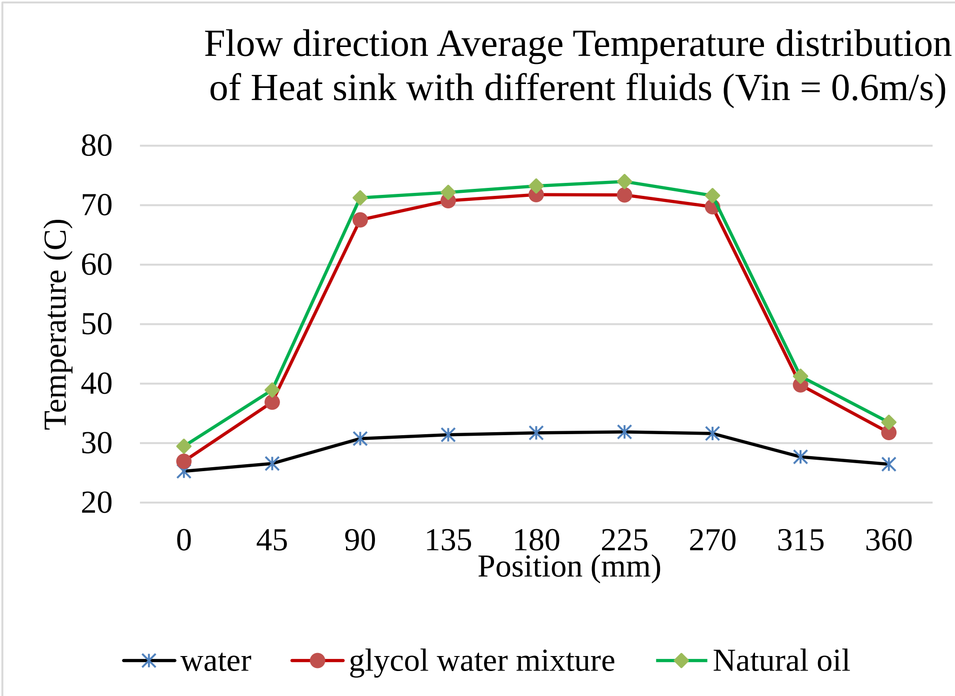

Figure 5.5. Flow Direction Heat sink Average Temperature comparison at Vin = 0.6m/s

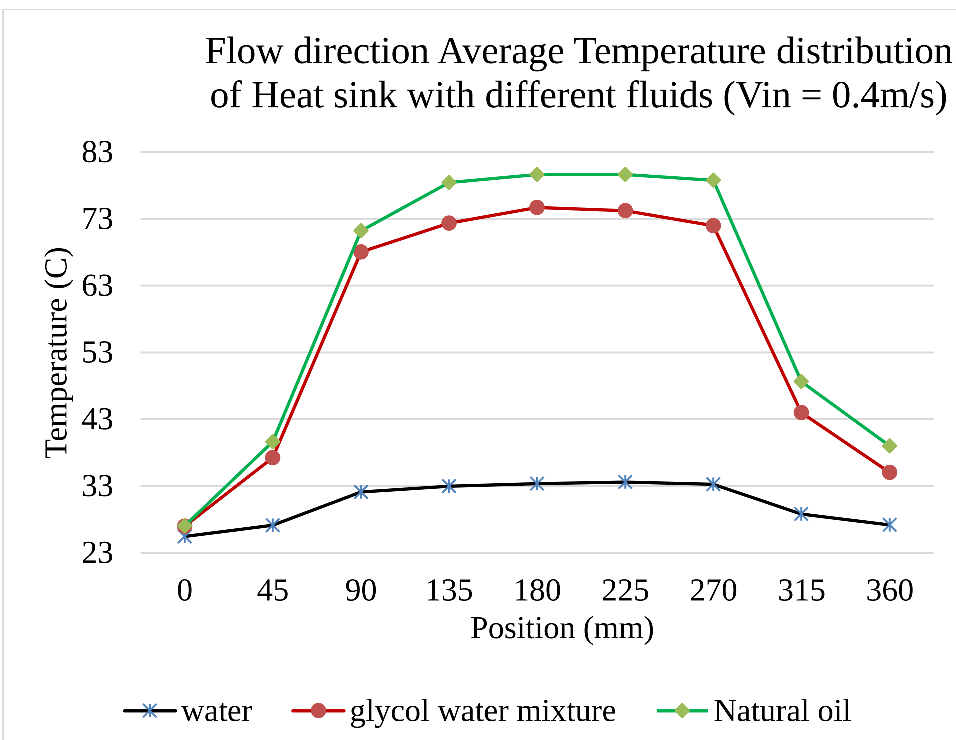

Figure 5.6. Flow Direction Heat sink Average Temperature comparison at Vin = 0.4m/s

5.2. Volume Average Heat Sink Temperature

The Volume Average Heat Sink Temperature showed that water had best cooling effect than the two other fluids to drop the target object's Temperature. At 0.8 m/s water cooled the Heat sink up to a a minimum Temperature of 31.17^{0}C while Heat sink cooled by Glycol water mixture with the same inlet velocity cooled to 32.92^{0}C. Natural Oil cooled the Heat sink up to an average of 45^{0}C.

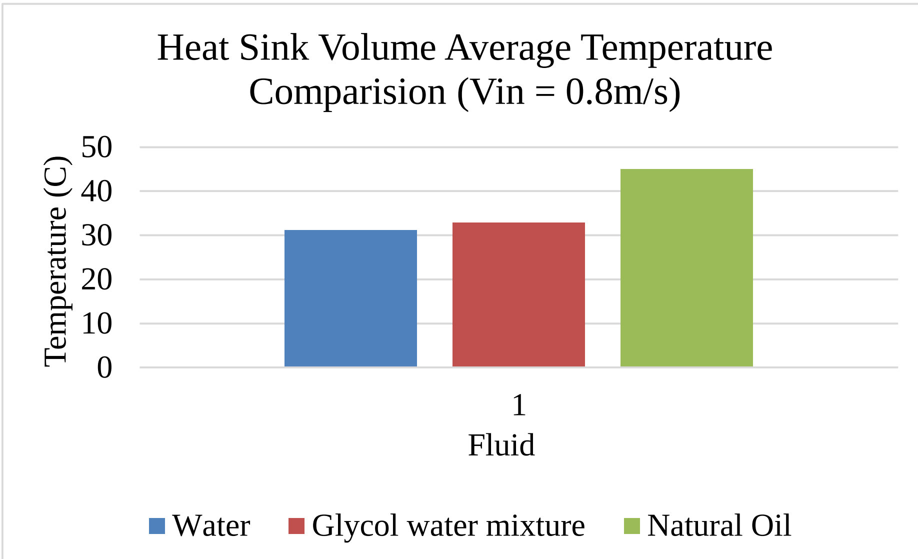

Figure 15.7. Heat Sink Volume Average Comparison at Vin = 0.8m/s

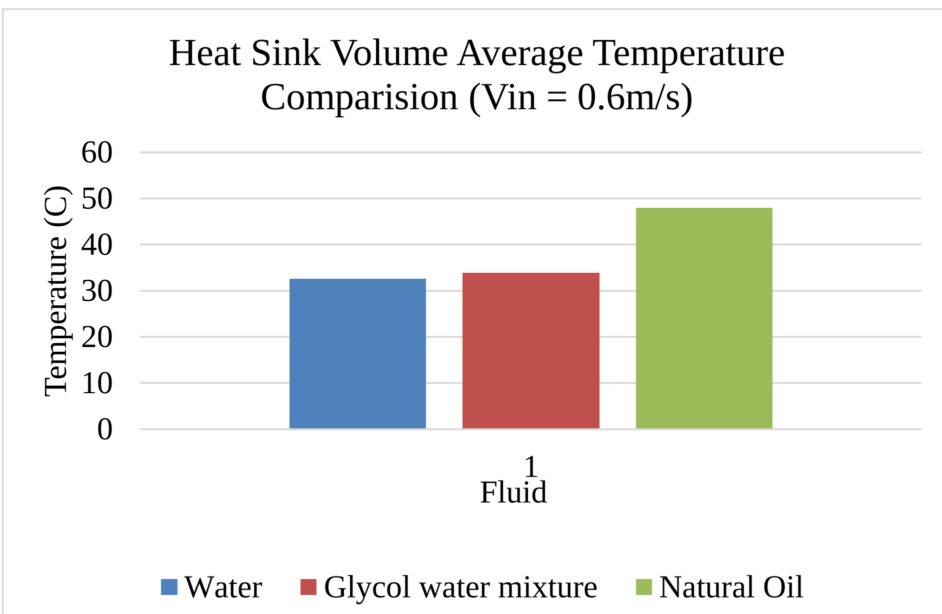

Figure 5.8. Heat Sink Volume Average Comparison at Vin = 0.6m/s

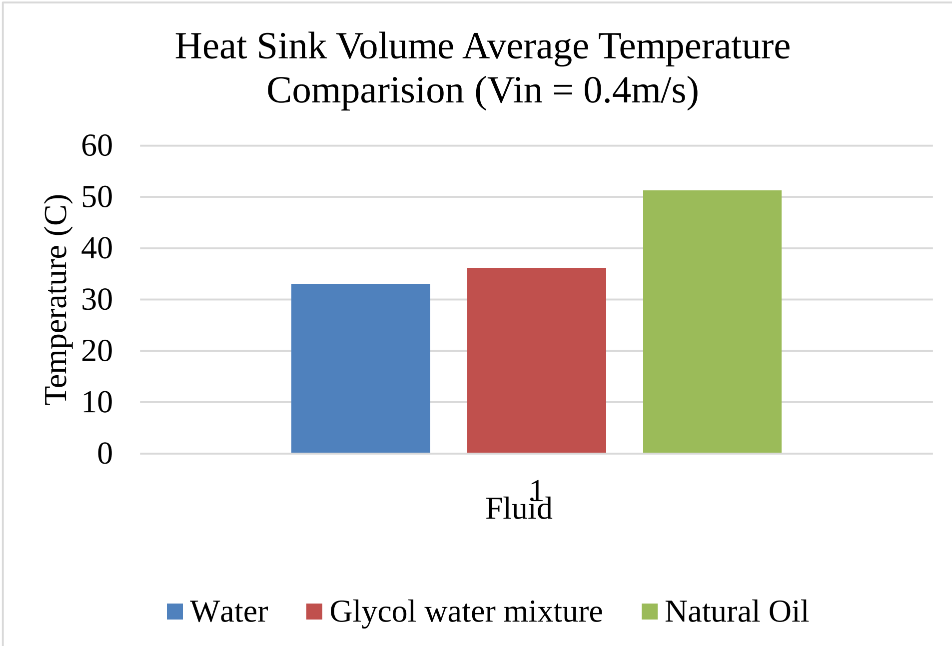

Figure 5.9. Heat Sink Volume Average Comparison at Vin = 0.4m/s

Pure water generally has a higher specific heat capacity than Glycol water mixtures and oil. It can absorb more heat per unit mass. Glycol water mixtures have better cooling properties than oil due to their higher specific heat capacity and thermal conductivity. They can absorb more heat per unit volume compared to oil, making them more effective coolants in many applications. Oil is generally less efficient at dissipating heat compared to Glycol-water mixtures and Pure water.

5.3. Analysis of Selected coolant (Water) with different Inlet Velocities

5.3.1. Heat Sink Temperature Comparison at different inlet velocities

The analysis of the flow field and temperature field was done at different fluid inlet velocities (which corresponds to the fluid's flow rate) and constant inlet temperature. Flow rate is directly affected by fluid velocity and flow area. As the geometry of the system is invariable, the only variable quantity is fluid inlet velocity. The more the fluid velocity is, the higher the fluid flow rate is.

Higher velocities cause the fluid flow to be more turbulent. This in turn results to an increase in heat transfer rate. 0.8m/s water inlet velocity resulted better cooling effect. It lowers the Temperature of the Heat sink. In the following figure, Vertical Heat sink average Temperature distribution comparison is presented at the three inlet velocities. It is the plot constructed from average Temperature values at different vertical heights of the Heat sink.

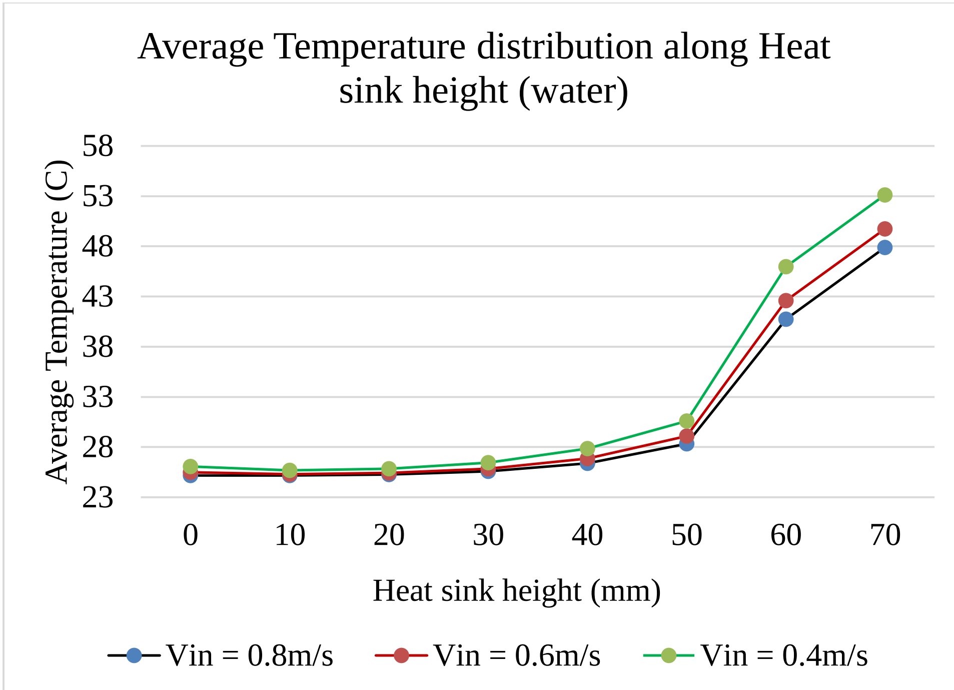

Figure 5.10. Vertical Heat Sink Average Temperature variation at different inlet velocities

The CFD result showed that, better cooling effect or lower Heat sink temperature is achieved at higher Velocities. At 0.8m/s inlet velocity, the Volume Average Heat sink temperature was about 31.17^{0}C. Fluid inlet velocities lower than this will result in an increase in temperature.

When going up to the top surface of the Heat sink. Average Temperature at different position varies. For 0.8m/s inlet velocity, it ranges from 25.18^{0}C to 47.88^{0}C from bottom surface up to top surface. A mass flow rate of 4.19Kg/s was recorded. This was conserved throughout the fluid flow positions. The total Heat transfer rate during this time was about 12960W.

A maximum of 64.58^{0}C occurred at the heat exposed surface (Top middle) of the Heat sink. This was the surface where 300000W/m^2 heat flux was directly applied from the Upper IGBT module. Heat was conducted in two dimension throughout the Heat sink.

The average top wall Temperature was reported as 47.88^{0}C. This surface is the area which has direct contact with heat generating equipment and need to be lower as much as possible.

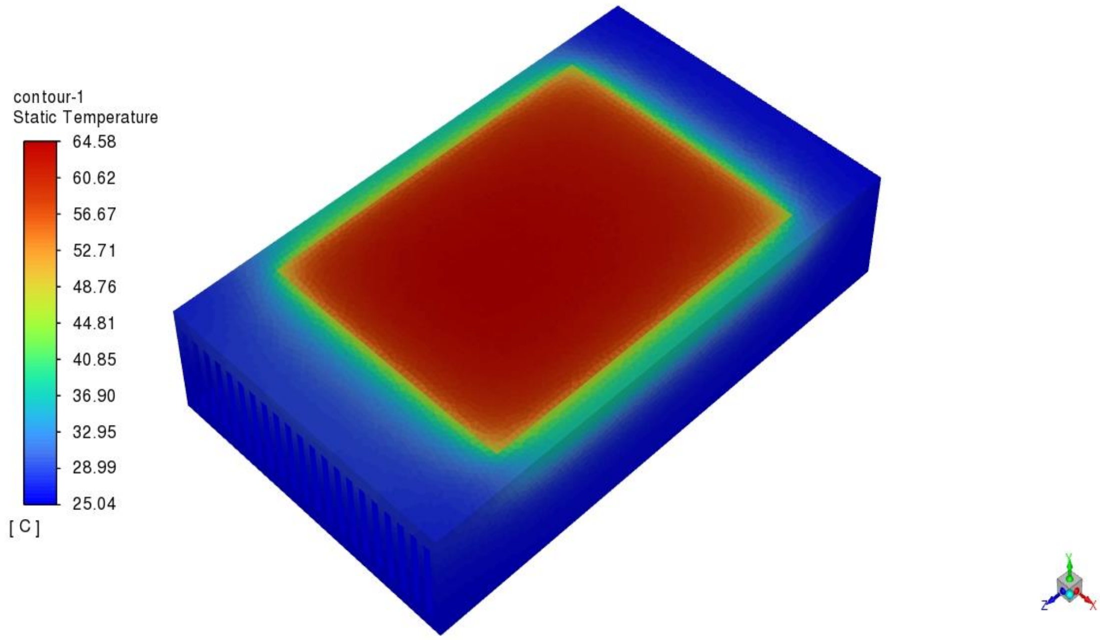

Figure 5.11. Heat sink Temperature Contour (V_{in} = 0.8m/s)

When decreasing water inlet velocity to 0.6m/s the average vertical Heat sink Temperature distribution showed increase in magnitude which was in between 25.49^{0}C and 49.7^{0}C. The maximum Top wall Temperature was 67.36^{0}C.

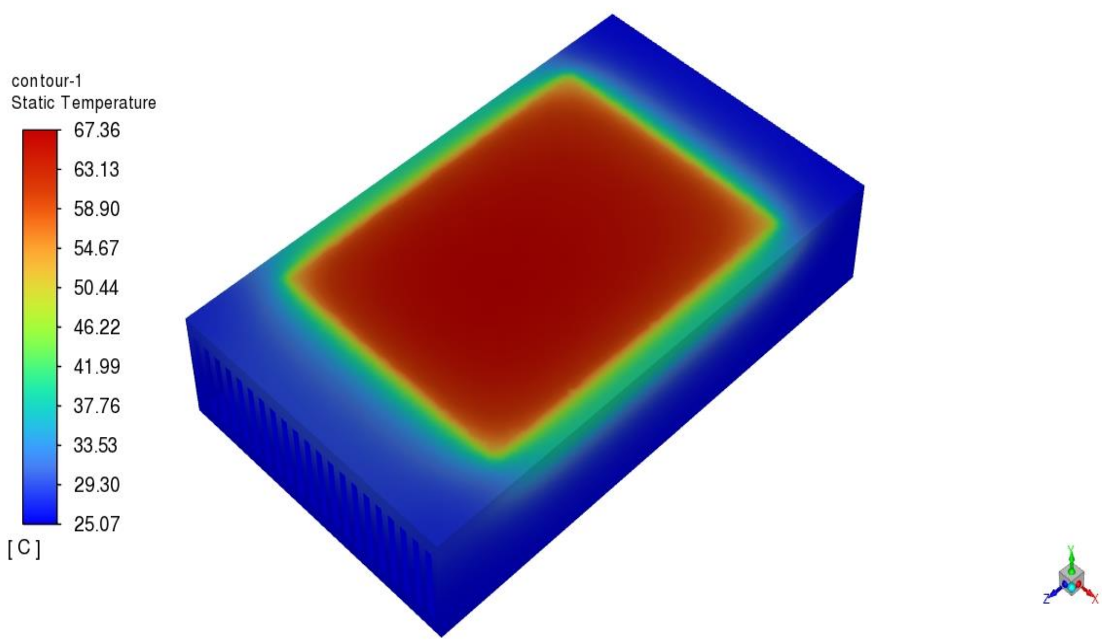

Figure 5.12. Heat sink Temperature Contour (V_{in} = 0.6m/s)

For water velocity inlet of 0.4m/s the Temperature range was from 26.07^0C to 53.12^0C. The maximum Temperature that occur at the top middle of the heat sink was 72.42^0C.

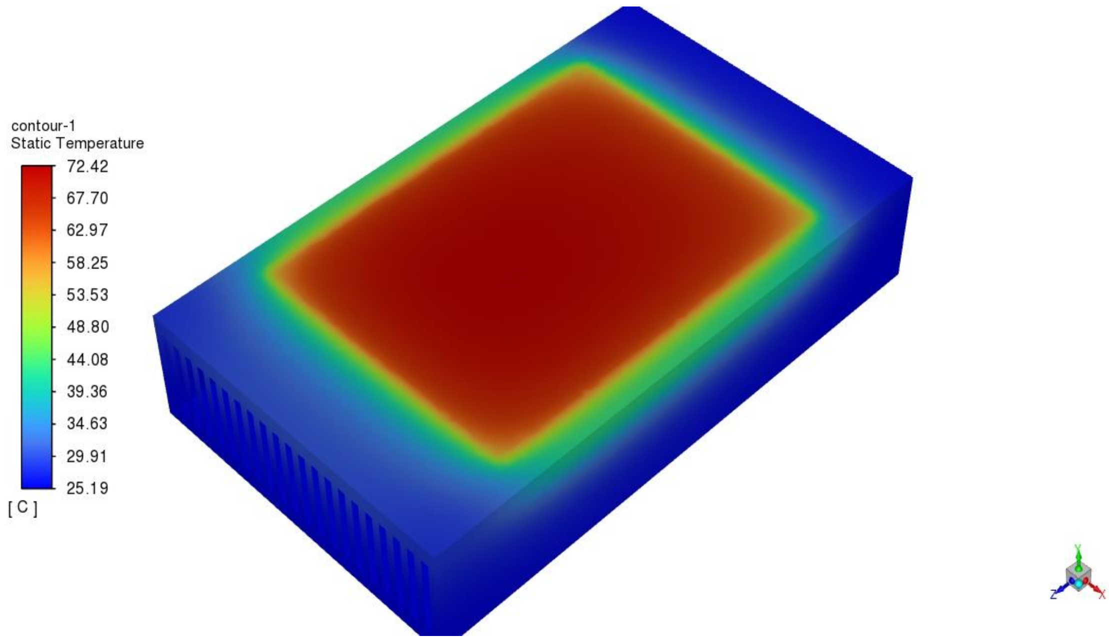

Figure 5.13. Heat sink Temperature Contour (V_{in} = 0.4m/s)

When going from inlet side to outlet side, the Heat sink Temperature slightly increased for the first millimeters and rises at the middle. It then dropped to its outlet temperature. Water flow with 0.8m/s showed relatively low temperature difference which made it best inlet velocity from others.

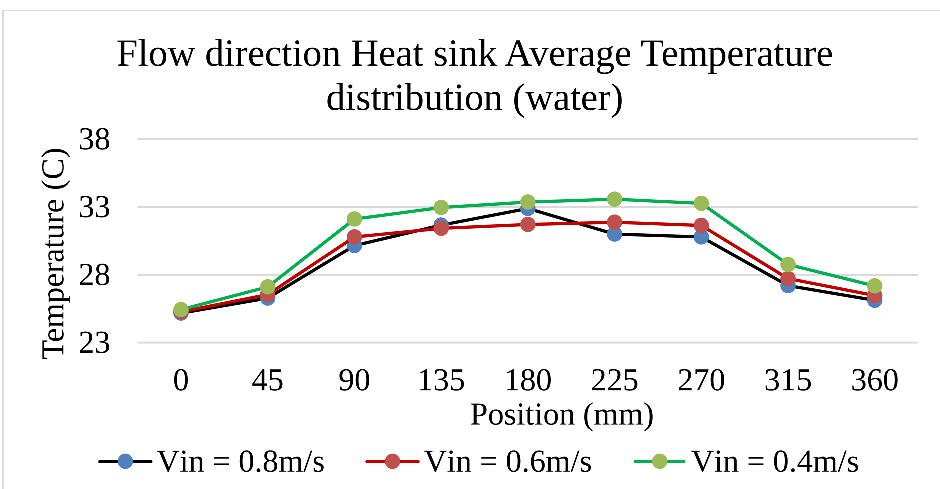

Figure 5.14. Flow direction Heat sink Average Temperature distribution

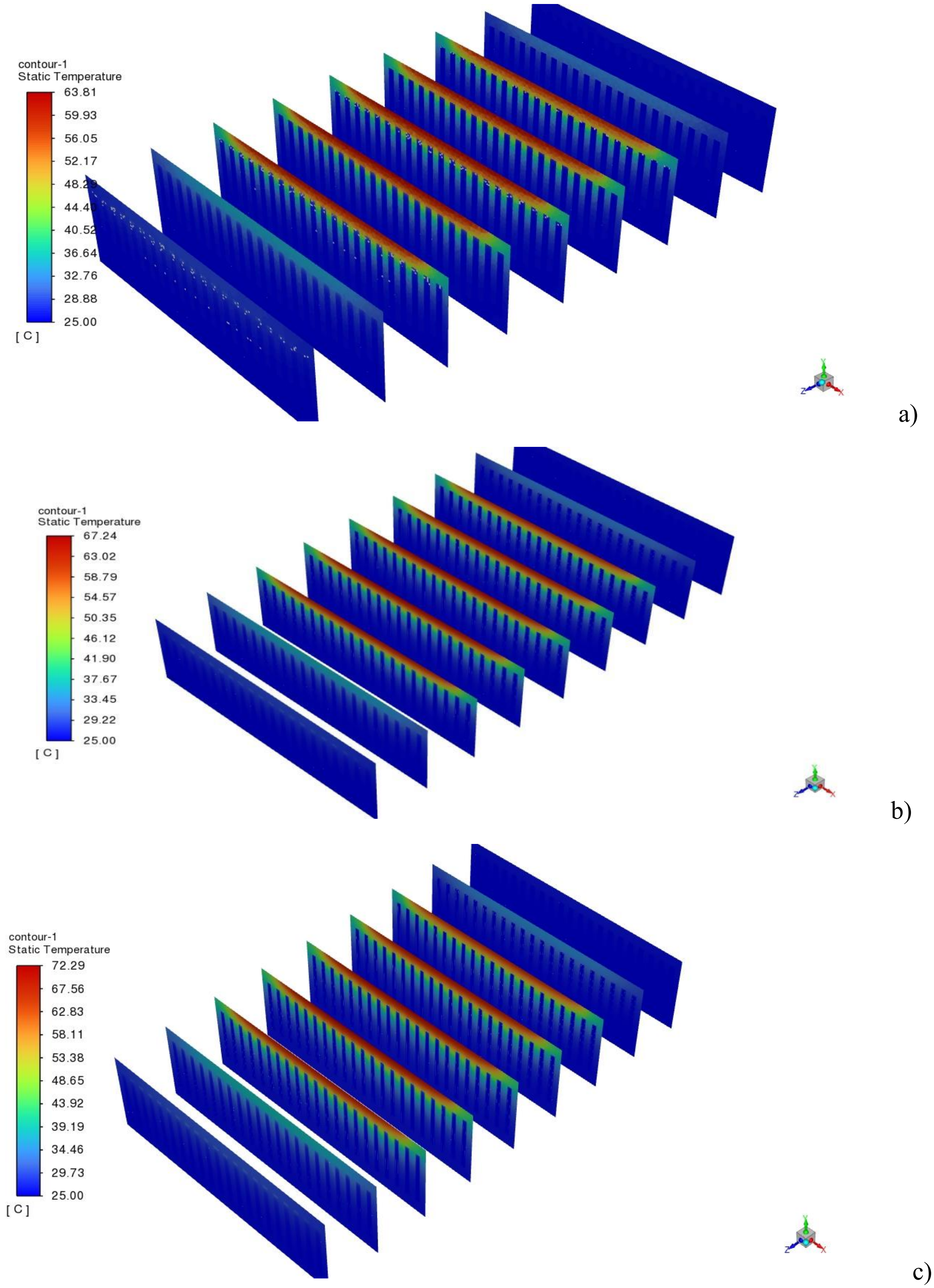

Figure 5.15. Temperature Contour along the flow direction a) Vin = 0.8m/s b) Vin = 0.8m/ c) Vin = 0.8m/

5.3.2. Temperature Distribution of the fluid

Near the inlet of the Heat sink, the cooling water assumed approximate temperature value as that of pump outlet. It then took off the heat energy from adjacent hot area and heated up. Around the Heat sink's outlet, the fluid temperature drops.

In this study, the temperature of fluid didn't show huge Temperature difference between the inlet and outlet ends. It is because of the availability of a number of flow channels (high fluid flow volume). Increasing fluid inlet velocity decreased the outlet velocity, since the time the fluid took to pass decreased at higher velocities.

Since no slip boundary condition was assigned at fluid solid interface, fluid assumed the same Temperature as its immediate wall Temperature (at y = 60mm). This was the maximum fluid temperature region.

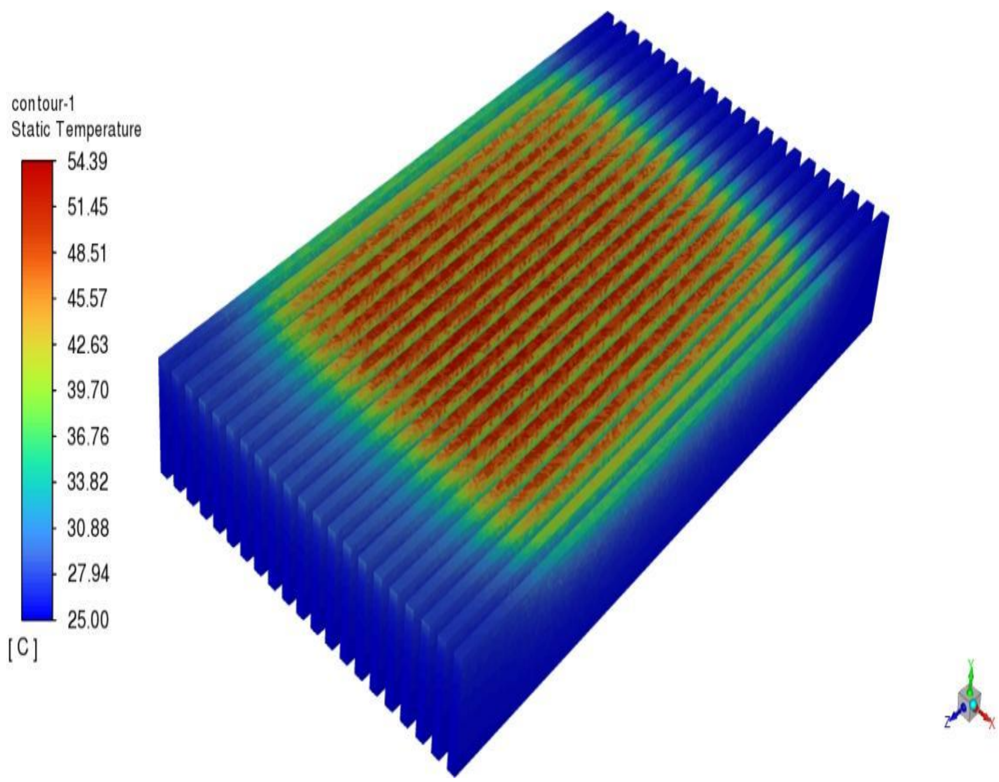

a)

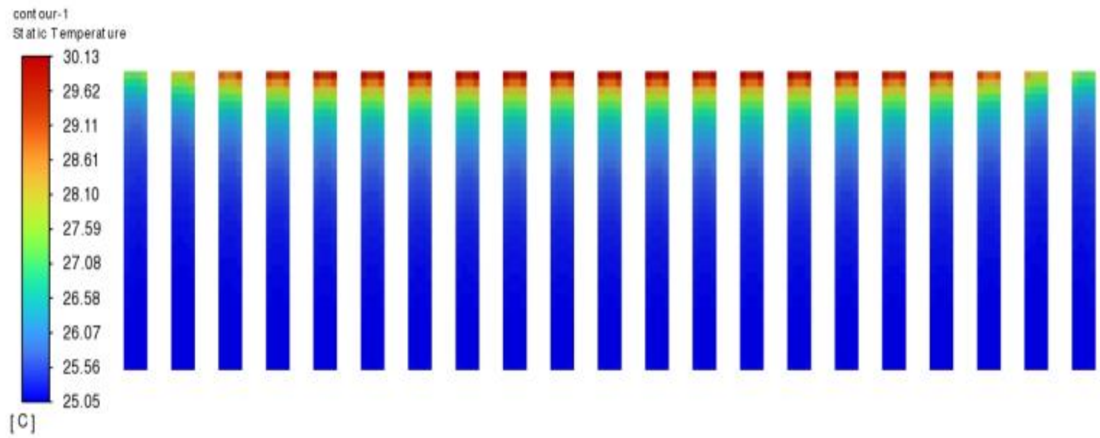

b)

Figure 5.16. Temperature contour of a) fluid domain b) fluid at outlet (Vin = 0.8m/s)

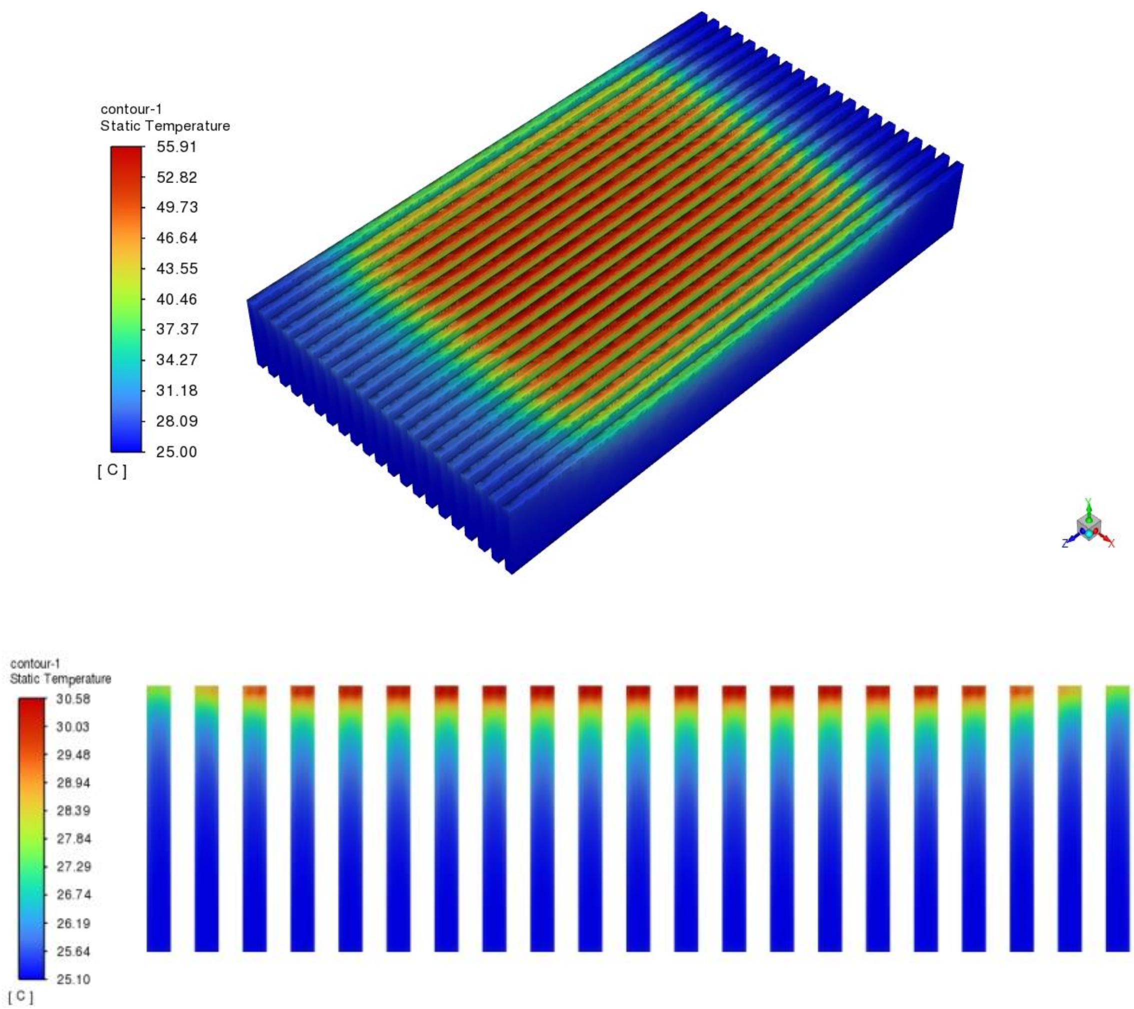

a)

b)

Figure 5.17. Temperature contour of a) fluid domain b) fluid at outlet (Vin = 0.6m/s)

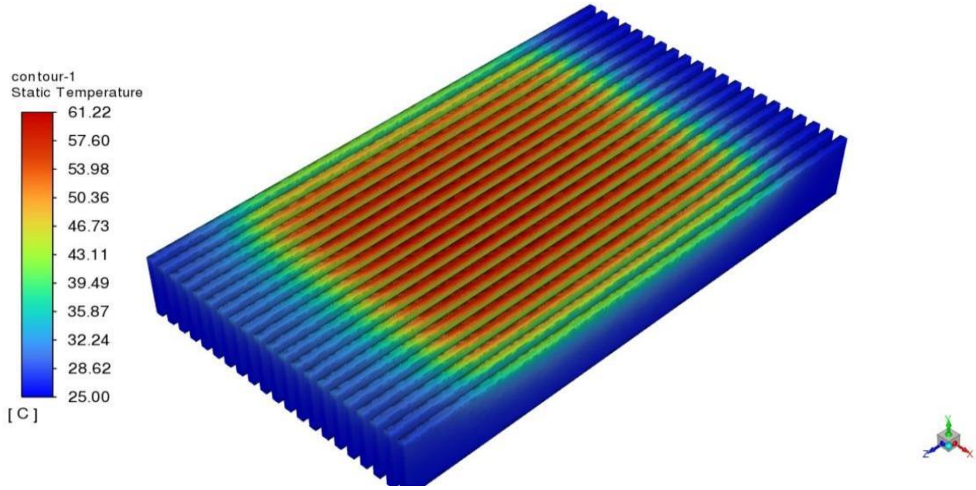

a)

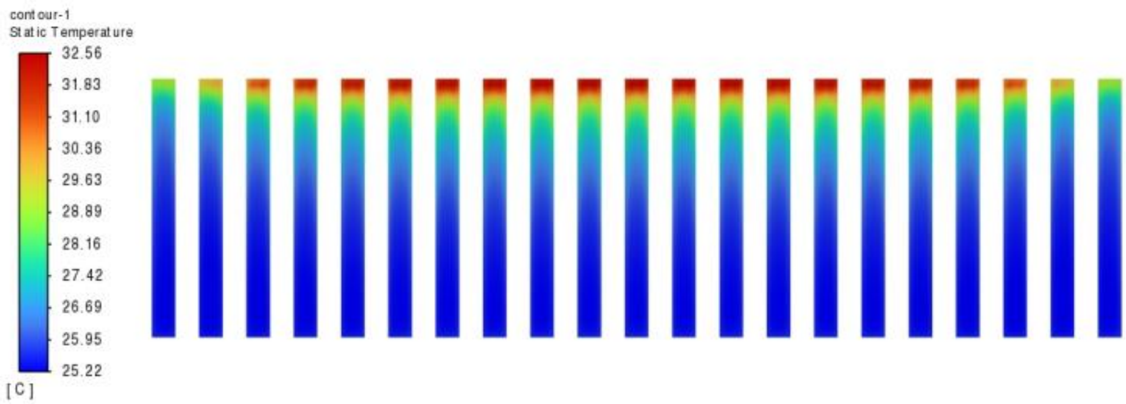

b)

Figure 5.18. Temperature contour of a) fluid domain b) fluid at outlet (Vin = 0.4m/s)

Table 5.1. Summary of Water cooled Heat sink comparison at different velocities

Physical Property	V_{in} = 0.8	V_{in} = 0.6	V_{in} = 0.4
Volume Average Temperature of Heat sink ((^{0}C)	31.17	32.05	33.8
Top wall Average Temperature (^{0}C)	47.88	49.74	53.12
Maximum top wall Temperature (^{0}C)	63.91	67.36	71.8
Maximum Fluid outlet Temperature (^{0}C)	30.13	30.58	33.35
Mass flow rate (Kg/s)	4.19	3.14	2.096
Rate of Heat transfer (W)	12960	12960	12960

According to the computational result, higher flow velocities experienced higher heat exchange and had relatively higher fluid outlet temperature. Increasing flow velocity more than this value can decrease the Heat sink temperature but increases pumping power and condenser sizing. Due to this fluid inlet velocity of 0.8m/s was selected as best velocity.

5.4. Comparison of Water cooled Heat sink with Air cooled Heat sink

Air was the existing cooling mechanism with inlet volume flow rate of $2.34 m^3/s$. Based on this the Numerical analysis of Heat sink with air as a fluid was performed and the following results were obtained.

Along the height, the average temperature of the Heat sink varies from 27.4^0C to 65.73^0C. The top surface has a maximum temperature of 90^0C at some point (heat exposed surface).

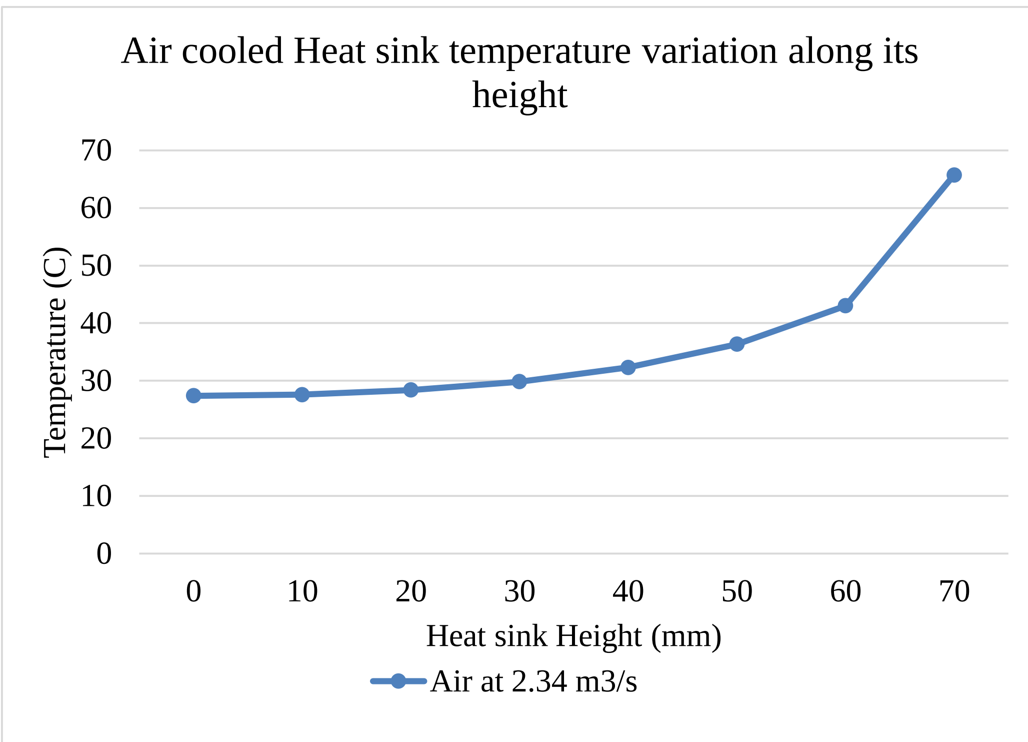

Figure 5.19. Vertical Average Temperature distribution of Air cooled Heat sink

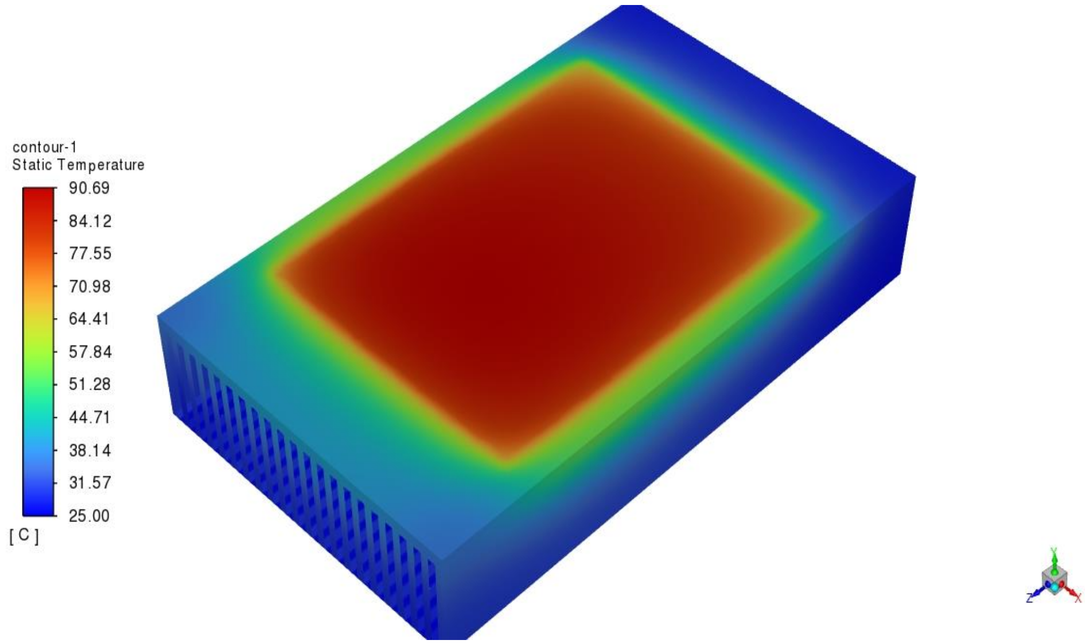

Figure 5.20. Air cooled Heat sink Temperature contour

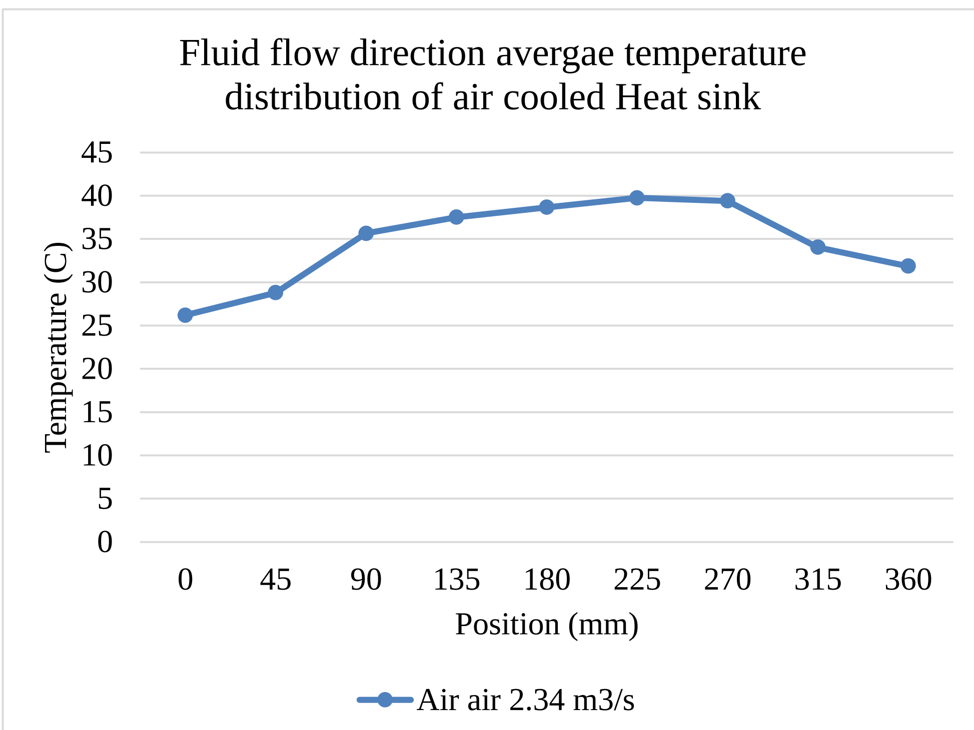

Figure 5.21. Flow direction average Temperature distribution of Air cooled Heat sink

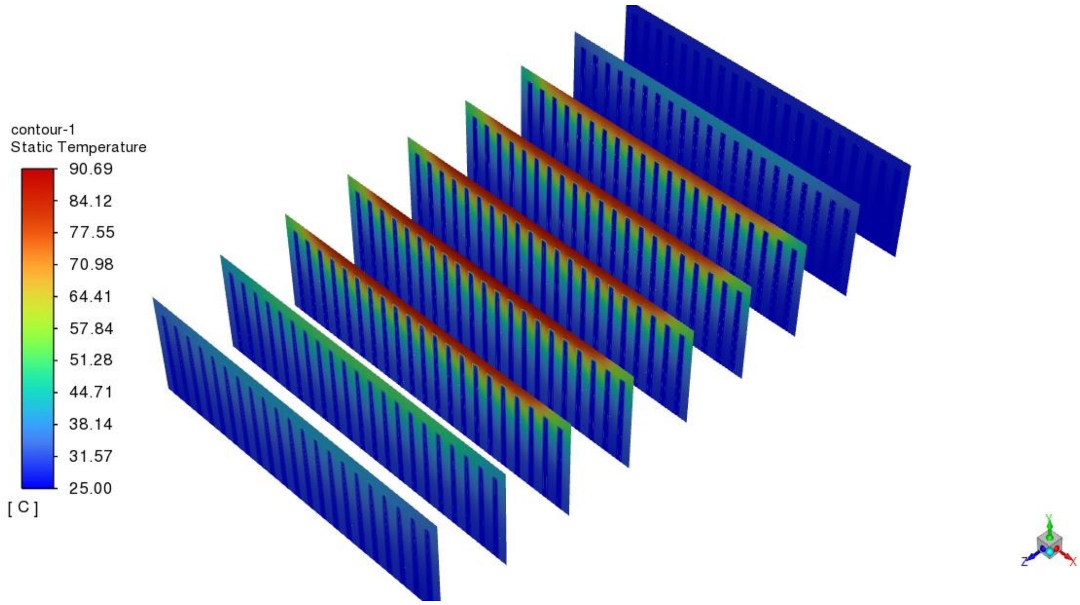

Figure 5.22. Flow direction Air cooled Heat sink Temperature contour

The fluid had 82.75^{0}C maximum temperature at its mid fluid solid interface. The outlet air Temperature has a maximum Temperature of 45.37^{0}C.

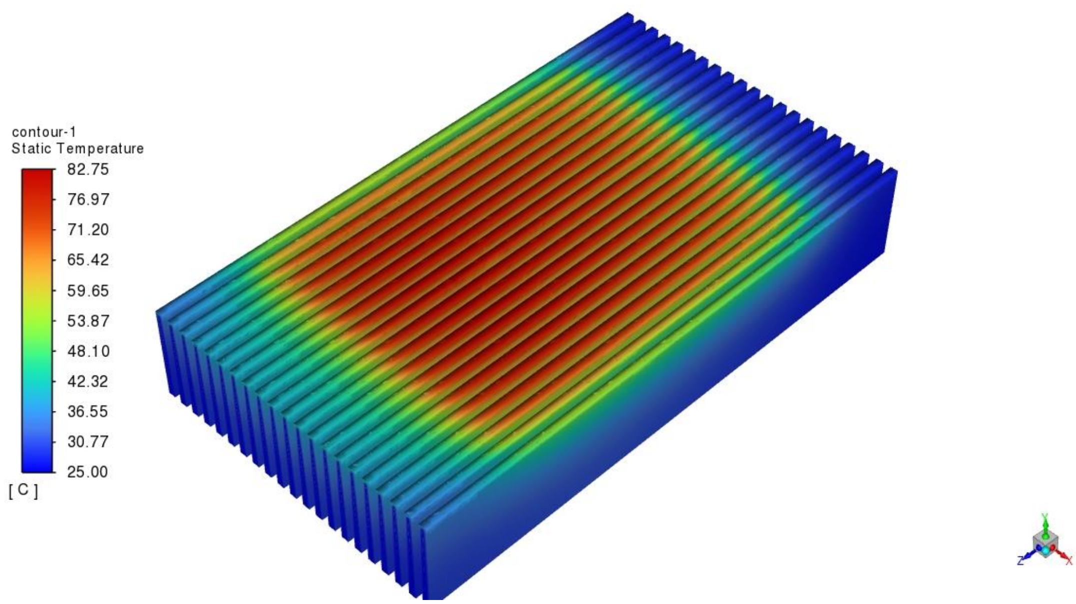

Figure 5.23. Fluid domain Temperature contour of Air cooled Heat sink

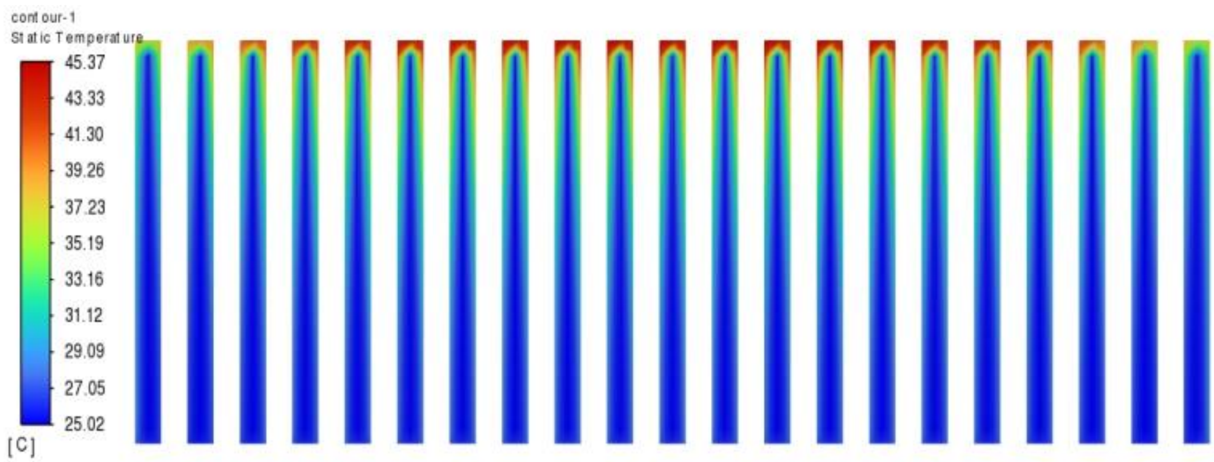

Figure 5.24. Fluid (Air) outlet temperature

Water is therefore the best coolant for Converter system cooling system than air and other coolants. Water is generally preferred to oil or glycol for heat dissipation.

The following table summarizes the advantage of using liquid (Water) over Air as Power Converter Heat sink coolant.

Table 5.2. Summary of Comparison of Air cooled Heat Sink Vs Water cooled Heat sink

Physical Property	Water at Vin = 0.8m/s	Air
Volume Average Temperature of Heat sink ((^{0}C)	31.17	42.02
Top wall Average Temperature (^{0}C)	47.88	65.73
Maximum top wall Temperature (^{0}C)	63.91	90.69
Maximum Fluid outlet Temperature (^{0}C)	30.13	49
Mass flow rate (Kg/s)	4.19	3.61
Rate of Heat transfer (W)	12960	12960

5.5. Mineral Composition of water

When selecting water as a working fluid, attention on its mineral composition must be given since dosed presence of some minerals affect its conductivity and maximize water corrosion.

Depending on its chemical composition, fresh water or tap water may cause rust formation in metals. Chloride, for example, which can usually be found in tap water is corrosive. Fresh water should not be used for a liquid cooling circuit if it contains more than 25 ppm of chloride or sulphates. The proportion of calcium and magnesium in water must also be observed, since both minerals cause lime scale on metal surfaces, thus reducing the thermal performance of the heat sinks (Arendt W. et. Al., 2015).

Table 5.3. Recommended upper limits for ions in cooling water

Minerals	**Recommended limit**
Calcium	< 50 ppm
Magnesium	< 50 ppm
Chloride	< 25 ppm
Sulphates	< 25 ppm

5.6. Collector Design

The Collector is a component of the liquid converter cooling system. It collects the fluid from each channel of the Heat sink at the outlet side and Delivers it to the main Return Pipe. At the inlet side, the same component is used to supply cold fluid to Heat sink with reverse Geometry.

It has two profiles that allow it to function as needed. The first rectangular section collects the whole fluid volume from each channel. The velocity of the fluid is expected to drop when entering the wider volume space. Simulation result of the Heat sink gave an average outlet velocity of almost the same as that of its inlet.

Total flow rate at the end of the heat sink (inlet of Collector) was obtained by considering the mass flow rate and density of the fluid. The average mass flow rate at the outlet of Heat sink was found from Simulation result which is 4.19Kg/s.

Based on Simulation result $V = \frac{m'}{\rho} = \frac{4.19}{998.2} = 0.0042\ m^3/s$.

This is equal with the value obtained by analytical method.

Based on Analytical Method $V = n \times A_i \times v = n \times (h \times w) \times v$

$= 21 \times (0.005 \times 0.05) \times 0.8 = 0.042 m^3/s$.

where n, A_i & v are number of flow channels, flow area and flow velocity respectively.

After the fluid leaves the 21 channels (with a total flow volume of $9 \times 10^{-5} m^3$) to the wider collector first section (with volume of $6.02 \times 10^{-4} m^{3)}$, its velocity drops to 0.34m/s. The second section of the collector is narrow and short outlet pipe with an internal diameter of 0.0381m. It has a length of 0.06m up to return pipe.

A geometry Design of the appropriate collector was done using ANSYS Design modeler and it was discretized with element size of 1mm for both the fluid and the solid part.

5.6.1. Fluent setup and input parameters for collector Analysis

Table 5.4. Input Parameters for collector Analysis

	Value	Unit
Overall Dimension of the collector	rectangular section (0.215 x 0.07 x 0.04 and Pipe section (0.0381 diameter & 0.06 length)	m (1 and 1/2 inch)
Inlet Velocity ($v_{i,c}$)	0.34	m/s
Inlet Mass flow rate (m'_c)	4.19	Kg/s
Rectangular portion Hydraulic Diameter (D_h)	0.106	m
Reynolds number based on inlet Velocity ($Re_{i,c}$)	35973	-
Inlet Temperature ($T_{i,c}$)	25.8	^0C

The numerical computation of the fluid flow was performed using ANSYS fluent with inlet boundary condition of 4.19Kg/s. the following table summarizes the fluent setup for collector simulation.

Table 5.5. Fluent setup for collector Analysis

Model	Turbulent (K-Omega, SST), Energy off	-
Fluid	Water	-
Inlet Boundary Condition	Mass flow inlet	4.19Kg/s
Outlet Boundary Condition	Pressure based	0Pa gauge pressure
Wall parts Boundary Condition	Adiabatic condition	-
Solution Method	Green Gauss cell based	-

5.6.2. Collector Analysis Results

As the water is Incompressible fluid, equal amount of fluid is expected to flow past any point of the collector in a specific time. This will assure conservation of mass or continuity of the flow. After the rectangular channel of the collector the fluid enters to a 0.038m diameter pipe.

The conservation of volume flow rate was checked Analytically by multiplying flow area and velocity at the two ends.

$$V_{i,c} = V_{o,c}$$

$$A_{i,c} \text{ x } V_{i,c} = A_{o,c} \text{ x } V_{o,c}$$

$$(0.205 \text{ x } 0.06) \text{ x } 0.34 = (3.14 \text{ x } 0.038^2/4) \text{ x } 3.8 = 0.0042 \text{ m}^3/\text{s}.$$

At the rectangular section the effective fluid flow area is (0.205 x 0.06) since the collector has a thickness of 0.005m.

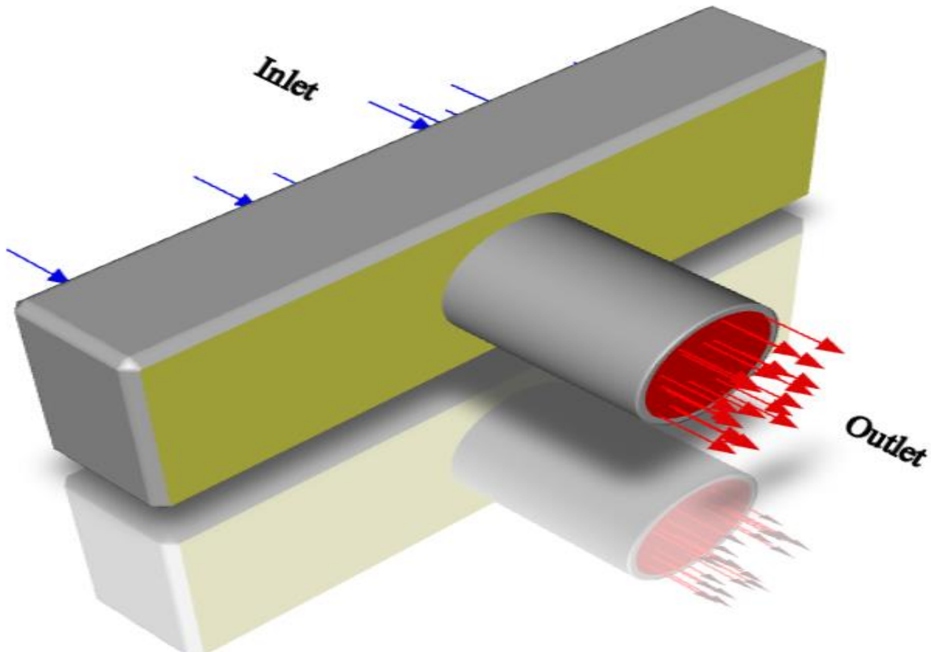

Figure 5.25. Boundary conditions of Collector

The mass flow rate was still conserved due to the increase in flow velocity even though the flow area was decreased. Temperature of the fluid is conserved since there is no heat generation and heat exchange with external environment.

Since flow area is narrower at the outlet than the inlet flow area, Fluid velocity boosted up to 3.8m/s. This kept the mass and volume flow rate of water equal with their inlet value. Mass flow rate of the fluid at the outlet was still 4.19Kg/s as expected. The Simulation result matched with the analytical one. That was $V = \frac{m'}{\rho} = \frac{4.19}{998.2} = 0.0042\ m^3/s$.

The velocity path line of the simulation showed that, the magnitude of fluid velocity increased after the second section of the collector (pipe portion). Some particles of the fluid had higher velocity at pipe inlet and outlet. However the average outlet fluid velocity was read around 3.8m/s.

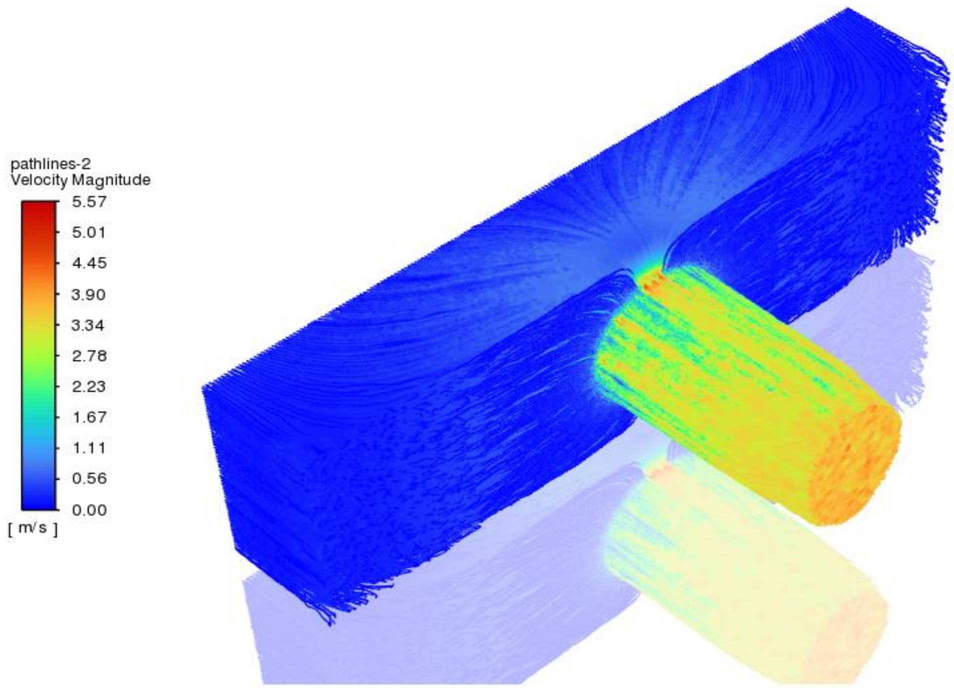

Figure 5.26. Velocity path line of Collector

Velocity vector helps to visualize the fluid flow around obstacles, depicting the details of the wake structure. The following image shows the fluid pattern at different geometry of the collector.

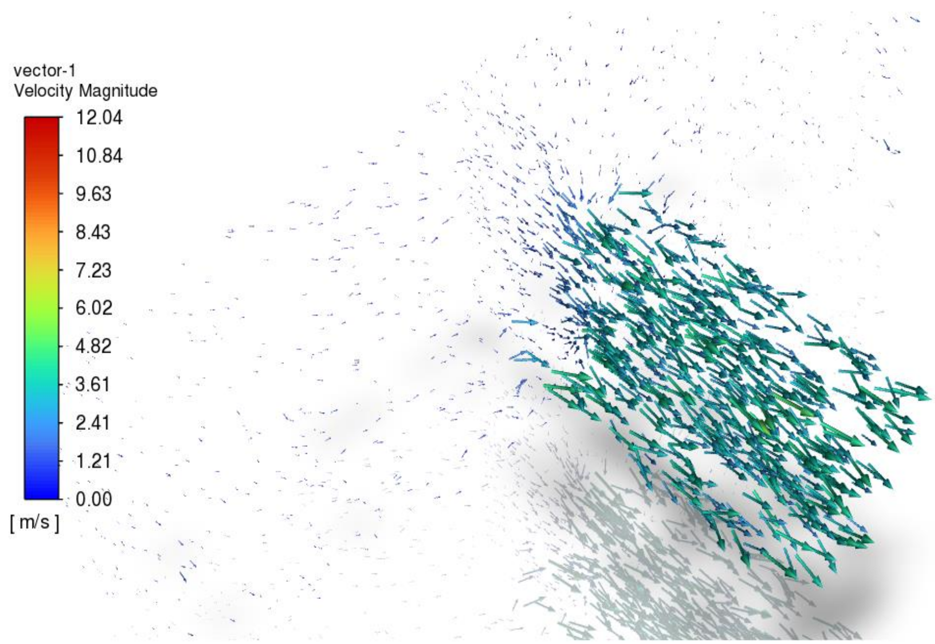

Figure 5.27. velocity vector of fluid flow inside collector

5.7. Return Pipe Design

The return pipe is the pipe that carries the hot fluid from one converter cabinet (i.e from 5 IGBTs and 1 Diode) to the condensing end. Including bends a single return pipe has a length of 1910mm. The cumulative outlet conditions of the collector are the input parameters for this pipe.

A total of Six Collectors supply hot fluid for this Return Pipe in parallel. The total volume flow rate through this pipe was the sum of the six Collectors flow rate.

$V_{total} = \sum_{i=1}^{n} Vi = V1 + V2 + V3 + \ldots + Vn$ for parallel pipe flow

$V_{i,rp} = \sum_{i=1}^{6} Vi = V1 + V2 + V3 + \ldots + V6 = = 0.0042 \text{ x } 6 = 0.0252 m^3/s$

Due to space limitation the size of Return pipe was limited to a standard nominal diameter of 300mm. The velocity of the collector exit was taken as an inlet velocity for the Return Pipe at six different sections.

Table 5.6. Input Parameters for Pipe Analysis

Parameters	Values	unit
Pipe Size ($D_{i,rp}$, L_{rp})	0.3 ID and 2.48 (including bent section)	m
Inlet Temperature (T_{rp})	30.13	^0C
Inlet Velocity ($V_{i,rp}$)	3.8	m/s

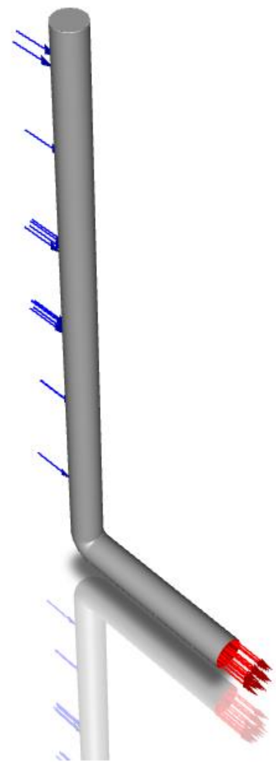

Figure 5.28. Return Pipe Geometry

At the end of the pipe a volume flow rate must be conserved. Using this volume flow rate and pipe diameter values, the velocity of fluid at the outlet of the pipe was determined.

$V = AV$ then for $D = 0.3m$ $v_{o,rp} = 0.35m/s$

5.8. Cold end Heat Exchanger Sizing

5.8.1. Heat Exchangers in General

To cool down the temperature of heat carrying fluid, another fluid with lower temperature must be introduced to it by means of Heat Exchanger. The fluids must be thermally in contact and must have a temperature difference between them. In some Heat Exchangers, fluids may be in direct contact while in others be separated by solid wall.

According to the fluid flow arrangement, Heat Exchangers are classified as Parallel flow, Counter flow and Cross Flow Heat Exchangers.

In parallel flow Heat Exchangers, the heat and cold fluids enter the exchanger at the same end, and flows in parallel to the exist end while in Counter Flow Heat Exchanger the two fluids enter from opposite ends, flow in opposite directions, and leave at opposite ends. The cold and hot fluids flow perpendicular to one another in Cross flow heat Exchangers.

5.6.2. Selection of Condenser Heat Exchanger

The water that enters the Heat sink was set as 25^0C. After cooling the target body, its outlet temperature raised by 5.13^0C. The volume of the Heat sink is larger when compared with the Heat exposed surface area. Only $0.0432m^2$ area (at the top) was exposed to heat flux. Out of $0.005418m^3$ Heat sink volume about $0.00025m^3$ was occupied by cooling fluid. About 21 rectangular channels were installed as flow passages. This all made the fluid temperature to have minimum temperature difference between the two ends.

The environment Temperature was taken as 25^0C. Based on this fact Cross Flow Heat Exchanger is valid choice for this system. The following section presents thermal and geometrical analysis of the Cross flow heat exchanger.

a. Primary Information

Table 5.7. Fluid properties for heat Exchanger sizing

Physical Property	Hot fluid	Cold Fluid
Hot fluid	Water	Air
Mass flow rate (Kg/s)	24.09	130
Inlet Temperature (^{0}C)	30.13	25
Outlet Temperature (^{0}C)	25 (desired)	? (to be calculated)
Specific heat Cp (J/Kg K)	4182	1006.43
Density (Kg/m^3)	998.2	1.225
Heat Exchanger material	Steel	

Assumptions in the Design of the Heat Exchanger

- The flow is steady state

- No phase change
- No heat leak to the environment
- No heat transfer in direction of flow

b. Required heat flux calculation

$Q_h = m \times cp \times (T_{hi} - T_{ho})$ hot fluid

$= 24.09 \times 4182 \times (30.13 - 25) = 516{,}818W$

$Q_c = m \times cp \times (Tc_0 - Tc_i)$ cold fluid

Since $Q_h = Q_c$

$516{,}818 = 130 \times 1006.43\ (Tco - 25)$ $Tc = 28.95^0C$

Log mean Temperature Difference (LMTD)

$\Delta Ti = Thi - Tci = 30.13 - 25 = 5.13$

$\Delta To = Tco - Tho = 28.95 - 25 = 3.95$

$LMTD = (\Delta Ti - \Delta To)/\ln(\Delta Ti/\Delta To) = 4.57$

Assuming $U = 1500W/m^2/k$

For correction factor

$P = (t2 - t1)/(T1 - t1) = (Tco - Tci)/(Thi - Tci) = (28.95 - 25)/(30.13 - 25) = 0.76$

$R = (T1 - T2)/(t2 - t1) = (Thi - Tho)/(Tco - Tci) = (30.13 - 25)/(28.95 - 25) = 1.29$

The correction factor corresponding to the above P and R values is 0.92

Then corrected Heat Transfer rate is

$Q = UFA(LMTD)$

$516{,}818 = 1500 \times 0.92 \times A \times 4.57$

Then Heat Transfer Area is $A = 81.9m^2$

And Length of Pipe was found as $A = 3.14 \times D_{rp} \times L$ $L = 87m$

5.9. Pump Selection

The available data that is helpful for pump selection is flow rate of fluid (water) and head desired to raise the fluid.

The Flow rate of the fluid was obtained from the inlet velocity (0.8m/s) and flow area ($0.00025m^2$). It was calculated in the previous section as $0.0042m^3/s$. The head desired is the sum of maximum IGBT and Diode layer in a single cabinet and the position of the Pump which is 4m.

$V = 0.0042m^3/s$ or $15.12m^3/hr$

H = 4m

Voltage = 380V

Frequency = 50Hz

The hydraulic pump power was obtained using the following formula.

$P_h = (V\ \rho\ g\ H) / (3600 \times 1000)$ in KW

Where P_h, V, ρ, g and H are representation for hydraulic power (kW), flow (m^3/h), density of fluid (kg/m^3), acceleration of gravity (9.81 m/s^2) and head (m) respectively.

$P_{h(kW)} = (15.12m^3/h \times 998.2\ kg/m^3 \times 9.81\ m/s^2 \times 4\ m) / (3600 \times 1000)$

$= 0.16KW$

Since two lines are needed, a pump power which is multiple of the above value is needed for the whole converter system (that is 0.32KW). It is possible to choose standard 0.5KW pump.

CONCLUSION AND RECOMENDATIONS

Conclusion

Numerical Analysis of three different fluids was performed for the thermal performance of heat sink. A steady state and velocity inlet boundary condition was taken for ANSYS fluent setup. The top wall of the Heat sink was exposed for a heat flux of 300000W/m^2 at its mid surface. Mineral Oil, Glycol water mixture with concentration of 50% (1:1) and pure water were the fluids under study for comparison. The following points can conclude the Numerical and Analytical results of the study.

- At selected fluid inlet velocities (0.4m/s, 0.6m/s & 0.8m/s) and inlet Temperature (25^{0}C), water was found to be best Power Converter Heat sink cooler as it has highest specific heat capacity.
- When using pure water as coolant at 0.4m/s, the Heat sink's volume average temperature was lowered to 33.8^{0}C and its top surface maximum temperature was decreased to 71.8^{0}C.
- At 0.6m/s water velocity, water cooled the volume of the heat sink up to the temperature of 32.05^{0}C and the surface exposed to the heat generating elements had a maximum temperature of 67.36^{0}C.
- The best (and the selected) water velocity choice was 0.8m/s. It was possible to achieve a maximum heat sink temperature (top surface) of 63.9^{0}C and volume average Temperature of 31.17^{0}C
- Water outlet maximum temperature at 0.8m/s reached 30.13^0 and this value was used for the next components analysis and sizing,
- A cross flow type condenser Heat exchanger (air and water) was used for the system having bend tube structure.
- Based on the available water flow rate and desired head, a pump with pumping power capacity of 0.16KW was selected.
- The selected Fluid (water) was compared with that of air cooling (existing system) and Water was found to cool the heat sink better. The minimum temperature that air can lower the Heat sink volume & top surface temperature was 42.02^{0}C and 65.73^{0}C respectively. It showed a Temperature decrease more than 10^{0}C on the heat sink.

- The Manufacturers manual specification about the Heat sink temperature just 2mm deep down the top surface was also used as a comparison to validate the analysis. As SEMIKRON's Technical Explanation manual, the top surface has a maximum temperature of 70^0C temperature to mm down the Heat sink top surface. This was even lower than the top surface temperature of the water cooled heat sink at 0.8m/s.

Recommendation(s)

Based on the present work and results the following recommendations are given for future works.

- Numerical Analysis of liquid cooling using transient time condition,
- Numerical Analysis and selection of Condenser heat exchanger, Piping system and Pump for the system and
- Experimental Analysis of Liquid cooled Converter System Heat sink using water as a cooling fluid,

REFERENCES

ANSYS Inc (2021). Ansys Fluent Theory Guide. http://www.Ansys.com

Ayhan Nazmi & Likani Ahmet (2022). Performance of parallel & Series channel cold plates used in Electric Vehicles by means of CFD simulations ESOGU Engin Arch Fac.2022,30(3), 397 404

Aranzabal, I., de Alegría, I. M., Delmonte, N., Cova, P., & Kortabarria, I. (2018). Comparison of the heat transfer capabilities of conventional single-and two-phase cooling systems for an electric vehicle IGBT power module. IEEE Transactions on Power Electronics, 34(5), 4185-4194. https://doi.org/10.1109/TPEL.2018.2862943

Arendt Wintrich, Ulrich Nicolai, Werner Tursky & Tobias Reimann (2015). Application Manual Semiconductors. SEMIKRON International GmbH. ISBN 978-3-938843-83-3 2nd revised edition

Dincer, I., Hamut, H., Javani, N. (2017). Thermal management of electric vehicle battery systems, John Wiley and Sons Ltd., United Kingdom. Retrieved from https://www.wiley.com/en- us.

Goldwind (2011). 1.5MW Wind Turbine Generator System Operation and Maintenance Manual (Vensys pitch, type I/II converter) Q/GW 2FW1500.44-2011

Haldkar, V., Sharma, A. K., Ranjan, R. K., & Bajpai, V. K. (2013). An energy analysis of condenser. International Journal of Thermal Technologies, 3(4), 120-125. http://inpressco.com/category/ijtt

Han, C. W., & Jeong, S. B. (2016). Evaluation of the thermal performance with different fin shapes of the air-cooled heat sink for power electronic applications. Journal of International Council on Electrical Engineering, 6(1), 17-25. https://doi.org/10.1080/22348972.2015.1115168

Han, F., Guo, H., & Ding, X. (2021). Design and optimization of a liquid cooled heat sink for a motor inverter in electric vehicles. Applied Energy, 291, 116819. https://doi.org/10.1016/j.apenergy.2021.116819

Haifeng, D., Ze-Chang, S., Xuezhe, W., Shugiang, Y.(2015). Design and simulation of liquid cooling plates for thermal management of ev batteries, EVS28, Kintex, Korea, 1, pp. 1-7. Retrieved from https://www.evs28.org/

He, L., Hu, X., Zhang, L., Xing, T., & Jin, Z. (2023). Performance Evaluation and Optimization of Series Flow Channel Water-Cooled Plate for IGBT Modules. Energies, 16(13), 5205. https://doi.org/10.3390/en16135205

Laloya, E., Lucia, O., Sarnago, H., & Burdio, J. M. (2015). Heat management in power converters: From state of the art to future ultrahigh efficiency systems. IEEE transactions on Power Electronics, 31(11), 7896-7908. https://doi.org/10.1109/TPEL.2015.2513433

Liang, J., Xu, H., Yuan, Z., & Zhou, P. (2020, June). High Efficiency Liquid Cooling System of Power Electronic Converter. In 2020 5th Asia Conference on Power and Electrical Engineering https://doi.org/10.1109/ACPEE48638.2020.9136363

Li, H., Ding, X., Jing, D., Xiong, M., & Meng, F. (2019). Experimental and numerical investigation of liquid-cooled heat sinks designed by topology optimization. International Journal of Thermal Sciences, https://doi.org/10.1016/j.ijthermalsci.2019.106065

Li, P., Luo, Y., Zhang, D., & Xie, Y. (2018). Flow and heat transfer characteristics and optimization study on the water-cooled microchannel heat sinks with dimple and pinfin. International Journal of Heat and Mass Transfer, 119, 152-162. https://doi.org/1016/j.ijheatmasstransfer.2017.11.112

Li, Y., Roux, S., Castelain, C., Fan, Y., & Luo, L. (2023). Design and Optimization of Heat Sinks for the Liquid Cooling of Electronics with Multiple Heat Sources: A Literature Review. Energies, 16(22), 7468.

Pan, M. (2021). Study of the performance of an integrated liquid cooling heat sink for high power IGBTs. Applied Thermal Engineering, 190, 116827. https://doi.org/10.1016/j.applthermaleng.2021.116827

SEMIKRON International (2017). Technical Explanation of SkiiP 4,PROMGT.1023. Rev 4

S. G. Kandlikar, W.J. Grande (2004) Evaluation of single phase flow in microchannels for high heat flux chip cooling thermohydraulic performance enhancement and fabrication technology, Heat Transfer Eng.

Silaipillayarputhur, K., & Khurshid, H. (2019). The design of shell and tube heat exchangers–A review. International Journal of Mechanical and Production Engineering Research and Development, 9(1), 87-102.

Šprlák, R., Kalvar, D., Opluštil, J., & Chlebiš, P. (2014, May). Design of experimental liquid heat sink for high power electronic. In 2014 14th International Conference on Environment and Electrical Engineering IEEE. https://doi.org/10.1109/EEEIC.2014.6835900

Unuvar, A., & Kargici, S. (2004). An approach for the optimum design of heat exchangers. International Journal of Energy Research, 28(15), https://doi.org/10.1002/er.1080

Vikram et al. (2013). An Energy Analysis of Condenser. International Journal of Energy Analysis,

Xiang Peng, Zhenyu Liu, Chan Qiu & Jianrong Tan (2014).Passage arrangement design for multi-stream plate-fin heat exchanger under multiple operating conditions Zhejiang University, Hangzhou Chaina. International Journal of Heat and Mass Transfer

Yijun et al. (2023). Design and Optimization of Heat Sinks for the Liquid Cooling of Electronics with Multiple Heat Sources: A Literature Review. MDPI Energies, 26

APPENDIX

A-1 Pure Water ANSYS Fluent results and Excel plots

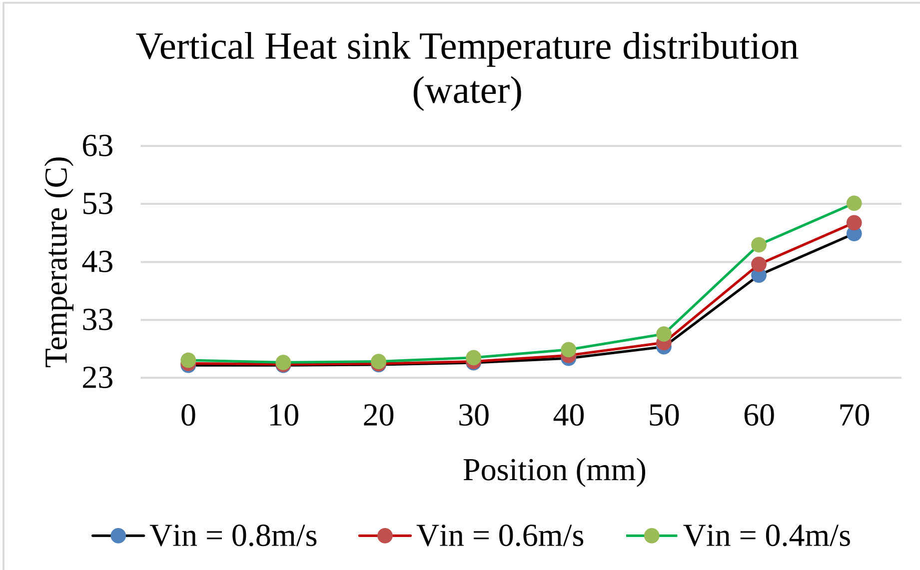

Figure: Temperature Distribution comparison along Heat sink's height (Water)

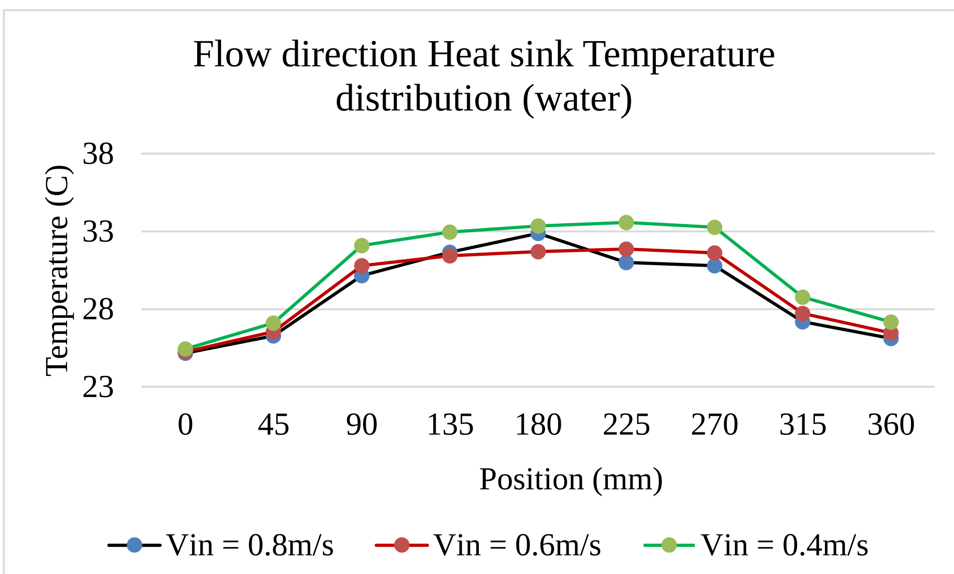

Figure: Temperature Distribution comparison along Fluid flow Direction (Water)

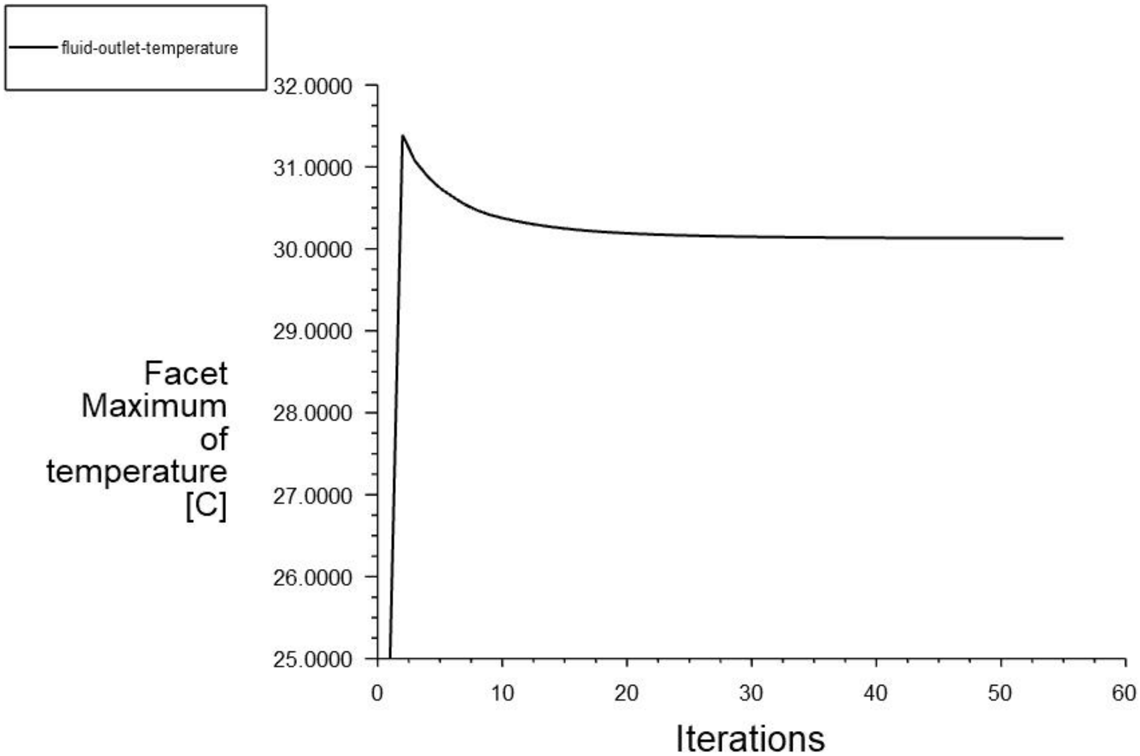

Figure: Outlet Temperature of water at v_{in} = 0.8m/s (Water)

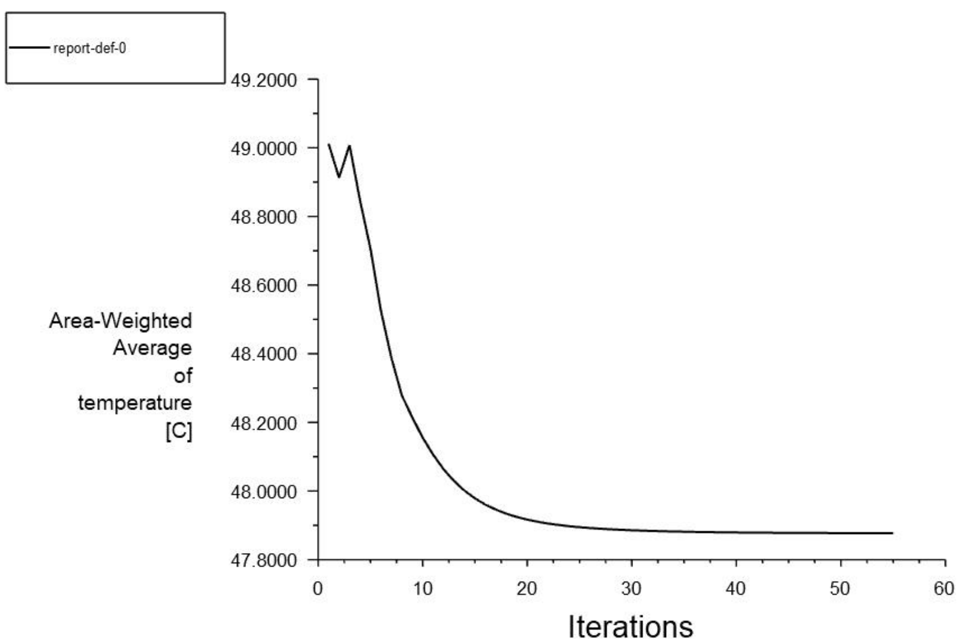

Figure: Top wall Temperature v_{in} = 0.8m/s (Water)

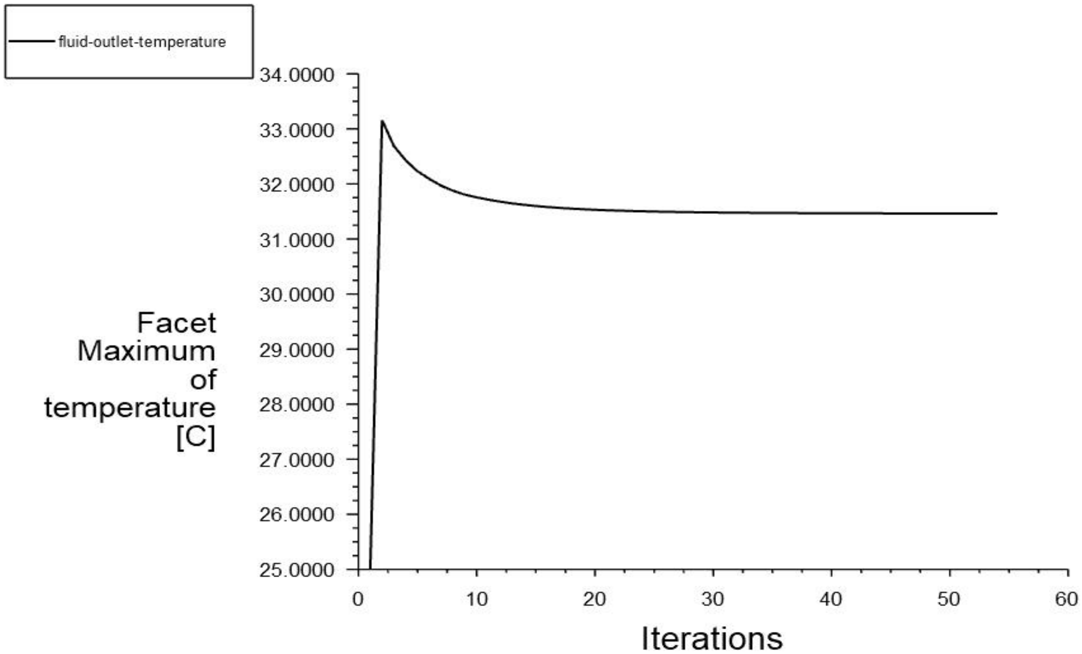

Figure: Outlet Temperature of water v_{in} = 0.6m/s (Water)

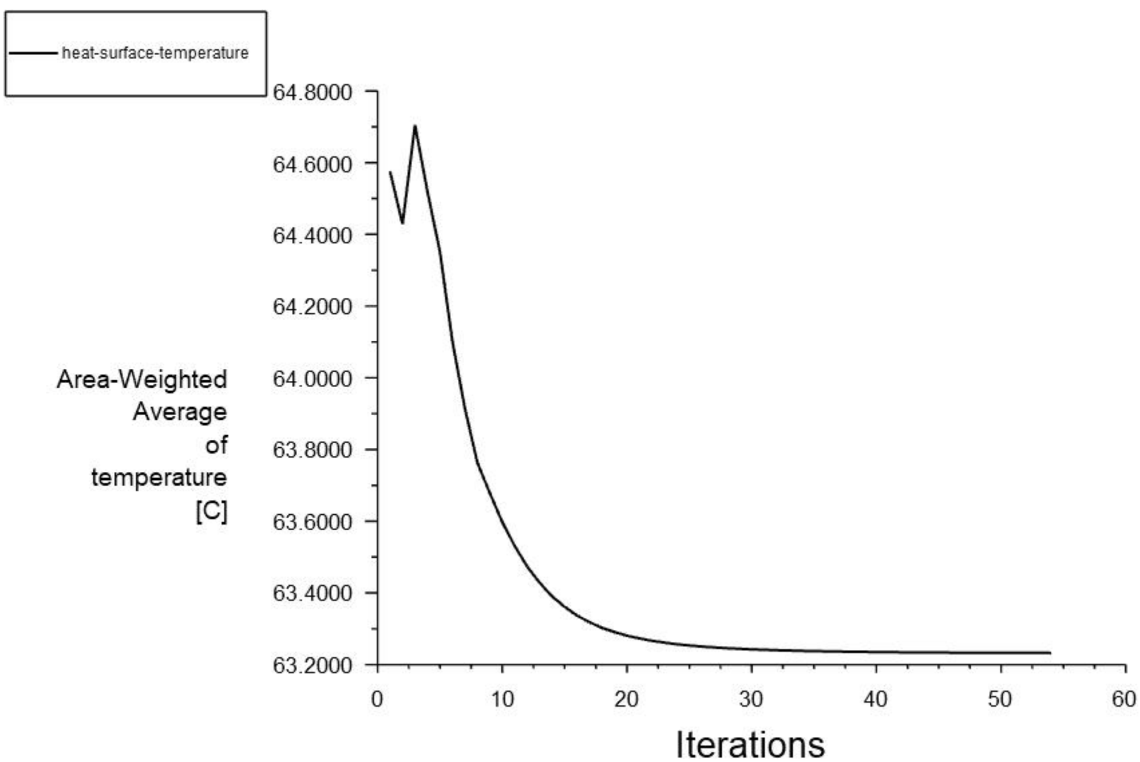

Figure: Heat Surface Temperature v_{in} = 0.6m/s (Water)

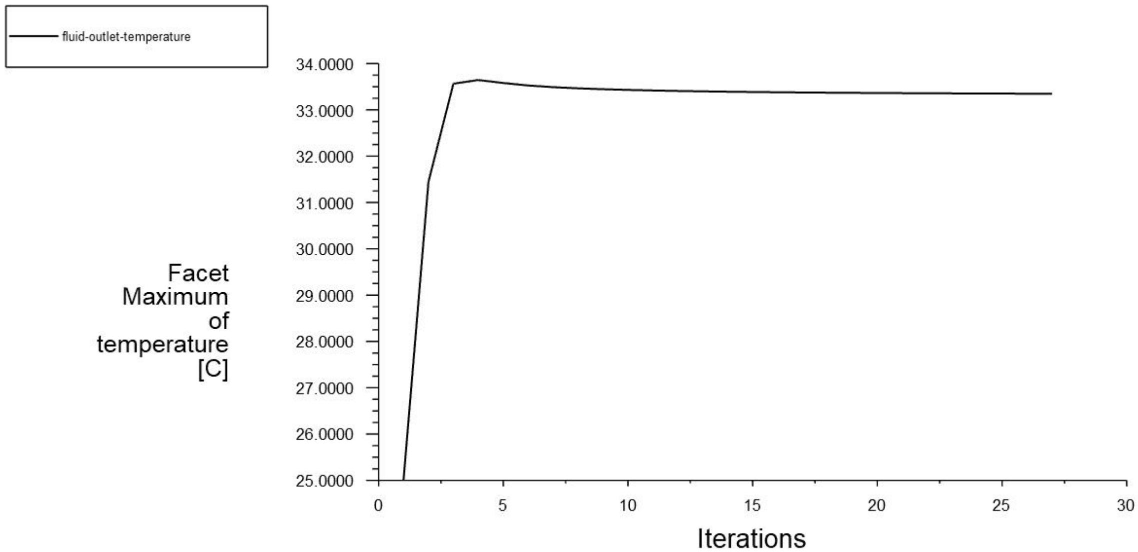

Figure: Outlet Temperature of water v_{in} = 0.4m/s (Water)

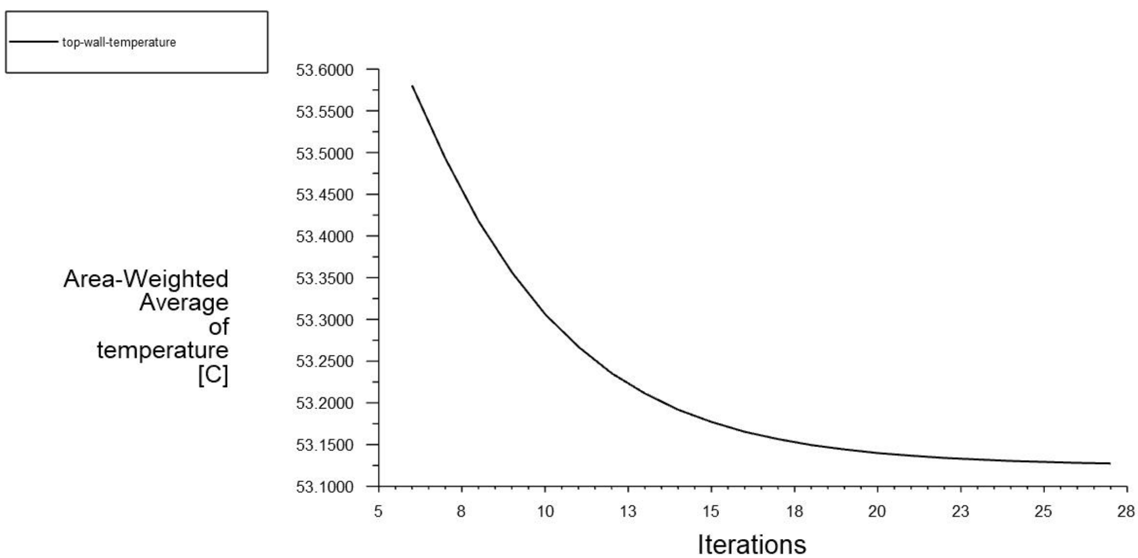

Figure: Top wall Temperature v_{in} = 0.4m/s (Water)

A-2 Glycol Water Mixture ANSYS Fluent results

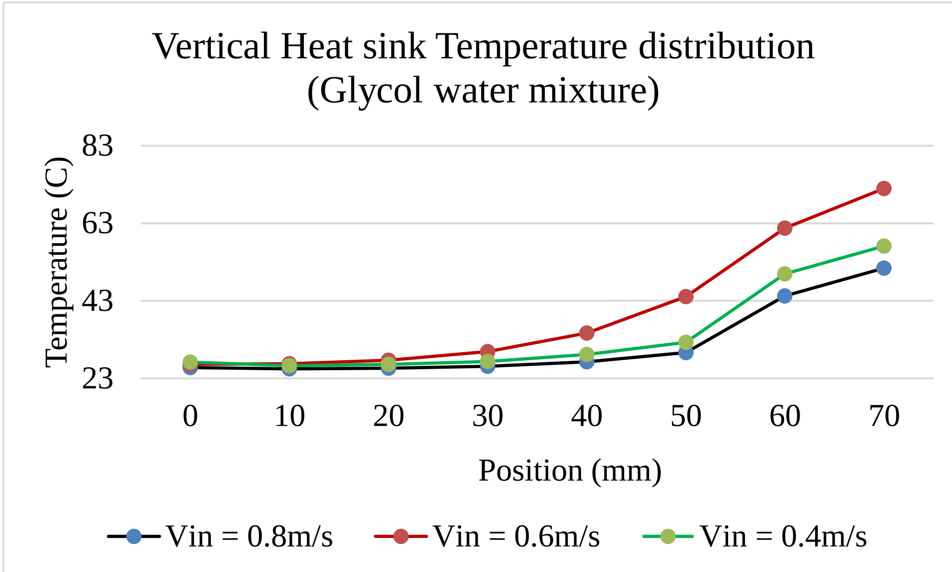

Figure: Temperature Distribution comparison along Heat sink's height (Gly-water mix)

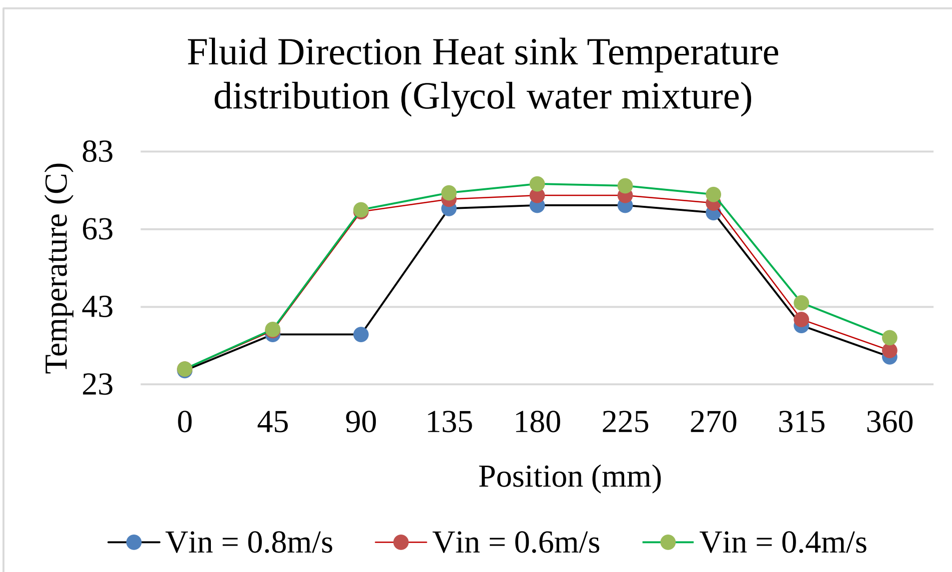

Figure: Temperature Distribution comparison along Fluid flow Direction (Gly-water mix)

A-3 Mineral Oil Mixture as a coolant ANSYS Fluent results

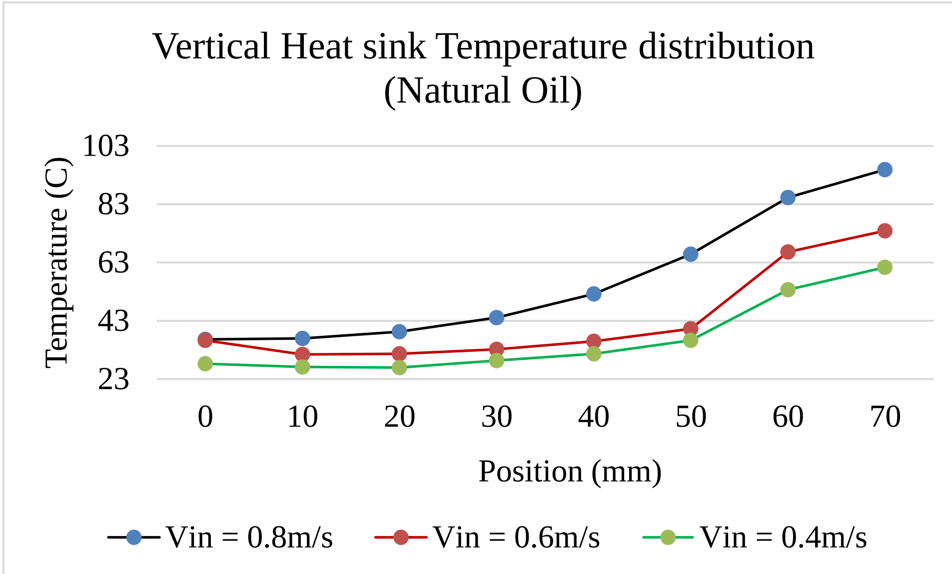

Figure: Temperature Distribution comparison along Heat sink's height (Mineral Oil)

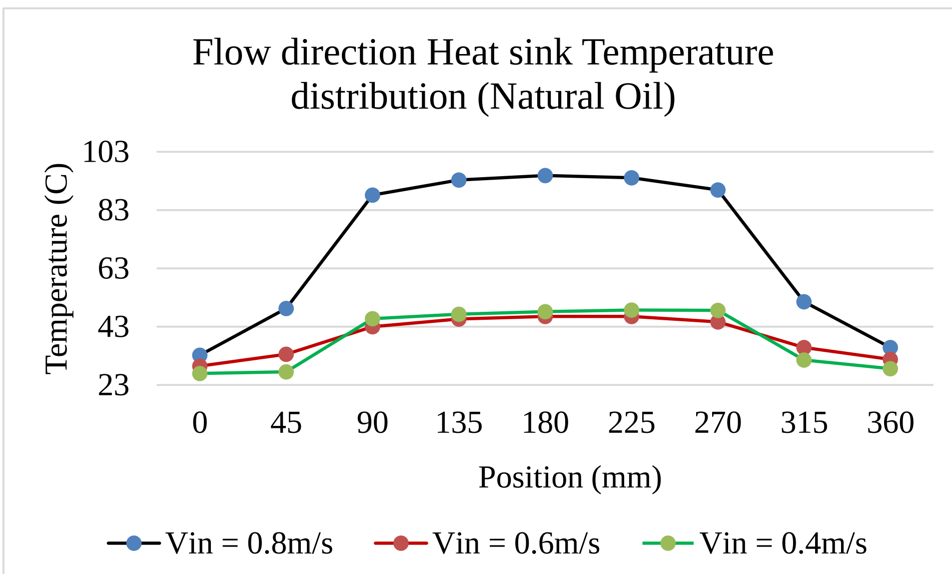

Figure: Temperature Distribution comparison along Fluid flow Direction (Mineral Oil)

A-4 Air as coolant ANSYS results

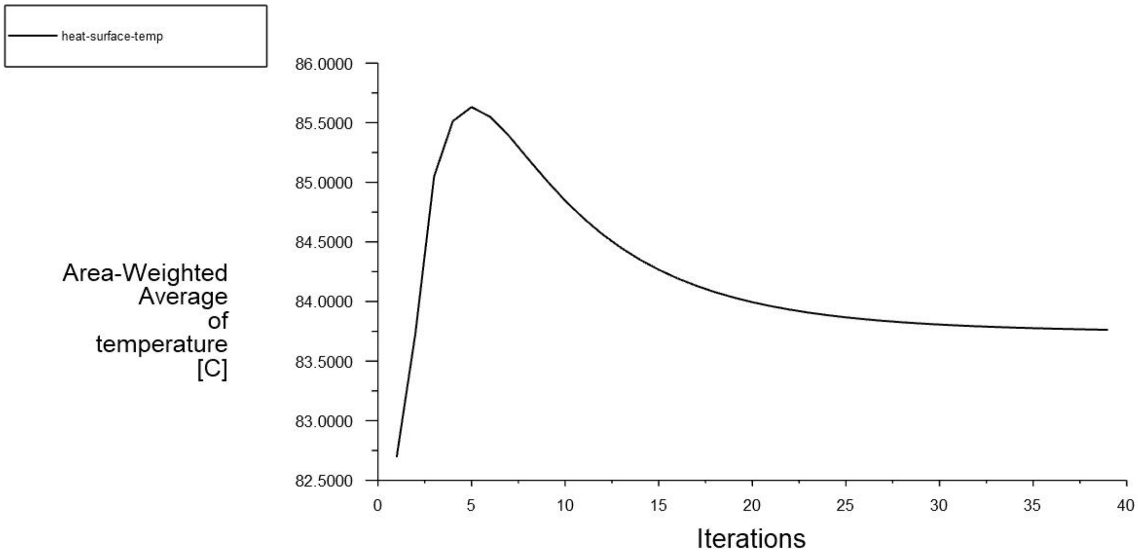

Figure: Heat Surface Temperature (Air)

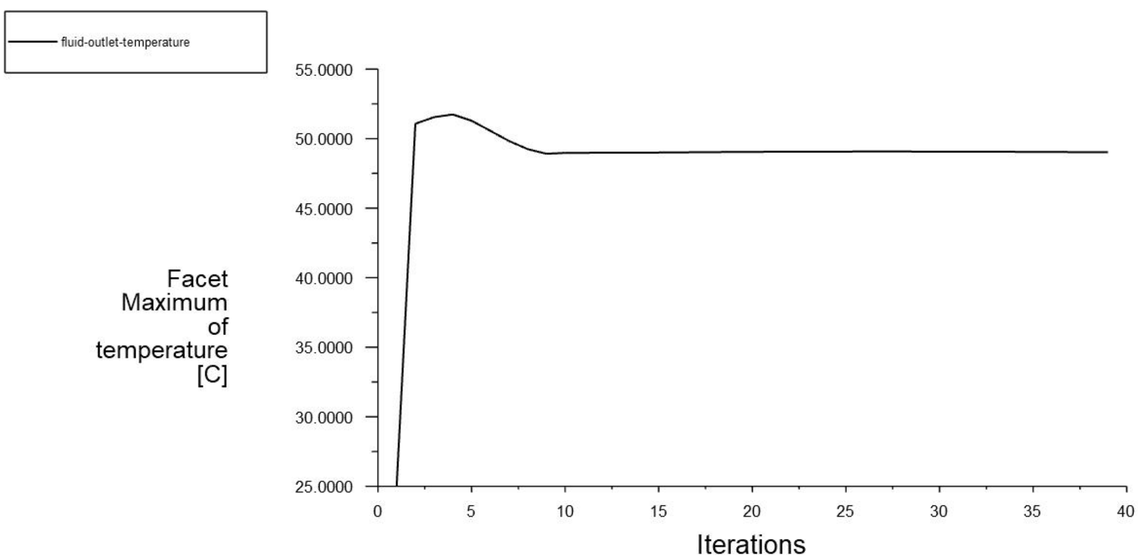

Figure: Fluid outlet Temperature (Air)

A-5 Manufacturer Data sheet

SKiiP 2414 GB17E4-4DUL V2

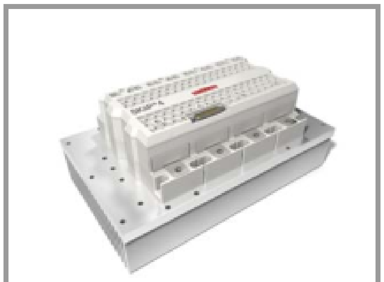

SKiiP® 4

2-pack-integrated intelligent Power System

SKiiP 2414 GB17E4-4DUL V2

Features*

- Intelligent Power Module
- Integrated current and temperature measurement
- Integrated DC-link measurement
- Solder free power section
- IGBT4 and CAL4F technology
- Safety isolated switching and sensor signals
- Digital signal transmission
- CAN Interface
- 100% tested IPM
- RoHS compliant
- UL file no. E242581

Absolute Maximum Ratings

Symbol	Conditions		Values	Unit
System				
V_{CC} 1)	Operating DC link voltage		1300	V
V_{isol}	DC, t = 1 s, each polarity		5600	V
$I_{t(RMS)}$	per AC terminal, rms, sinusoidal current		500	A
$I_{max\ (peak)}$	max. peak current of power section		3600	A
I_{FSM}	T_j = 175 °C, t_p = 10 ms, sin 180°		15885	A
I^2t	T_j = 175 °C, t_p = 10 ms, diode		1262	kA^2s
f_{out}	fundamental output frequency (sinusoidal)		1	kHz
T_{stg}	storage temperature		-40 ... 85	°C
IGBT				
V_{CES}	T_j = 25 °C		1700	V
I_C	T_j = 175 °C	T_s = 25 °C	3385	A
		T_s = 70 °C	2723	A
I_{Cnom}			2400	A
T_j 2)	junction temperature		-40 ... 175	°C
Diode				
V_{RRM}	T_j = 25 °C		1700	V
I_F	T_j = 175 °C	T_s = 25 °C	2362	A
		T_s = 70 °C	1869	A
I_{Fnom}			2400	A
T_j 2)	junction temperature		-40 ... 175	°C
Driver				
V_s	power supply		19.2 ... 28.8	V
V_{iH}	input signal voltage (high)		V_s + 0.3	V
dv/dt	secondary to primary side		75	kV/µs
f_{sw}	switching frequency		10	kHz

Figure: Semikron Skiip 4 IPM Data Sheet